

1
2
3
4
5
6
7
8
9
10
11
12
13
14
15
16
17
18
19
20
21
22
23
24
25
26
27
28
29
30
31
32

Coordination of rooting, xylem, and stomatal strategies explains the response of conifer forest stands to multi-year drought in the Southern Sierra Nevada of California

Junyan Ding^{1,2}, Polly Buotte³, Roger Bales⁴, Bradley Christoffersen⁵, Rosie A. Fisher^{6,7}, Michael Goulden⁸, Ryan Knox¹, Lara Kueppers^{1,3}, Jacquelyn Shuman⁶, Chonggang Xu⁹, Charles D. Koven¹

1. Climate and Ecosystem Sciences Division, Lawrence Berkeley National Lab, Berkeley, USA
2. Pacific Northwest National Lab, Richland, WA, USA
3. Energy and Resources Group, University of California, Berkeley, USA
4. Sierra Nevada Research Institute, University of California, Merced, USA
5. Department of Biology, University of Texas, Rio Grande Valley, USA
6. Climate and Global Dynamics Division, National Center for Atmospheric Research, Bold, USA
7. Laboratoire Évolution & Diversité Biologique, CNRS:UMR 5174, Université Paul Sabatier, Toulouse, France
8. Dept. of Earth System Science, University of California, Irvine, USA
9. Earth and Environmental Sciences Division, Los Alamos National Laboratory, Santa Fe, New Mexico, USA

Corresponding author: Junyan Ding (junyan.ding@pnnl.gov)

Key Points:

- We perform a sensitivity analysis using the model FATES-Hydro to explore the coordination of leaf, xylem, and root hydraulic traits of pine in Southern Sierra Nevada.
- We find that rooting depth is the major control on water and carbon fluxes, and that deep-rooted pines with risky stomata have the highest GPP but also the highest drought mortality risk.
- Resolving both the plant water sourcing strategies and subsurface processes are critical to represent drought impacts on conifer forests.

33
34
35
36
37
38
39
40
41
42
43
44
45
46
47
48
49
50
51
52
53
54
55
56
57

Abstract

Extreme droughts are a major determinant of ecosystem disturbance, which impact plant communities and feed back to climate change through changes in plant functioning. However, the complex relationships between above- and belowground plant hydraulic traits, and their role in governing plant responses to drought, are not fully understood. In this study, we use a plant hydraulic model, FATES-Hydro, to investigate ecosystem responses to the 2012-2015 California drought, in comparison with observations, for a site in the southern Sierra Nevada that experienced widespread tree mortality during this drought.

We conduct a sensitivity analysis to explore how different plant water sourcing and hydraulic strategies lead to differential responses during normal and drought conditions.

The analysis shows that:

- 1) deep roots that sustain productivity through the dry season are needed for the model to capture observed seasonal cycles of ET and GPP in normal years, and that deep-rooted strategies are nonetheless subject to large reductions in ET and GPP when the deep soil reservoir is depleted during extreme droughts, in agreement with observations.
- 2) risky stomatal strategies lead to greater productivity during normal years as compared to safer stomatal control, but lead to high risk of xylem embolism during the 2012-2015 drought.
- 3) for a given stand density, the stomatal and xylem traits have a stronger impact on plant water status than on ecosystem level fluxes.

Our study reveals the importance of resolving plant water sourcing strategies in order to represent drought impacts on plants, and consequent feedbacks, in models.

58 **1. Introduction**

59 Understanding plant water use strategies and the resulting ecohydrologic processes in
60 forests is critical for predicting surface water and energy exchange, carbon dynamics and
61 vegetation dynamics of water-constrained ecosystems in a changing climate. Mediterranean-
62 type climates, as in California, are characterized by dry and hot summers and cool, wet winters,
63 resulting in asynchronous supplies of energy and water. In addition to these climatic stresses,
64 plants in California are further subject to high inter-annual variability in precipitation, and
65 periodic severe drought events, such as the recent 2012 – 2015 drought, which led to widespread
66 tree mortality (Fettig et al. 2019). Together, these two climatic constraints bring a unique
67 challenge to the success of forests in California, which are likely to be exacerbated in a warming
68 climate.

69 On evolutionary timescales, natural selection has led to a wide array of strategies and
70 functional traits that allow plants to both grow and survive under a range of environment
71 conditions (Grime 1977,1979; Coley et al. 1985; Westoby et al. 2002; Craine 2002; Reich et al.
72 2003). Given the centrality of water sourcing on plant physiology, plant hydraulic traits play an
73 important role in water-constrained ecosystems. Once absorbed by fine roots, water flows
74 through the vascular system via coarse roots, stems, branches, to leaves where it evaporates
75 through stomata. The rate of water flow through stems, and thus the supply to leaves, is
76 determined by the hydraulic conductivity along this pathway. If the water potential of xylem
77 tissue becomes too low, cavitation can occur and cause a loss of conductivity. Because this
78 cavitation can damage the xylem network, trees have developed different strategies to mitigate
79 this effect, all of which come at some cost. These strategies include 1) early stomatal closure or
80 leaf deciduousness to reduce the flow of water, at the cost of reduced carbon intake; 2) building
81 cavitation-resistant xylem, at the cost of increased hydraulic resistance; and 3) growing deep
82 roots to access more moisture, at the cost of higher carbon investment. In this study, we focus on
83 the potential hydraulic strategies that trees in Californian ecosystems use, with a particular
84 emphasis on how the co-ordination of hydraulic functional traits at the leaf, stem, and root levels
85 is critical to carbon assimilation, transpiration, and consequently, the productivity and the
86 response of trees to drought (Matheny, Mirfenderesgi, and Bohrer 2017; Matheny et al. 2017;
87 Mursinna et al. 2018a).

88 The traits that regulate stomatal conductivity are the most important hydraulic traits of
89 leaves and the primary ones through which photosynthesis and transpiration are coupled.
90 Stomatal behavior falls along a gradient between two extremes: stomata may close early during
91 water stress to avoid the risk of hydraulic failure, or remain open to maximize carbon uptake
92 while exposing xylem to a higher risk of embolism (Martínez-Vilalta, Sala, and Piñol 2004;
93 McDowell et al., 2008; Skelton, West, & Dawson, 2015, Matheny et al. 2017). The sensitivity of
94 stomata to water stress determines where the stomata operate along the safety-risky gradient, and
95 thus the degree that carbon intake is traded for preventing the cavitation of xylem. Where the
96 best stomatal strategy sits along the safety-risky gradient would depend on the physical
97 environment.

98 The maximum hydraulic conductivity and the vulnerability to cavitation are the two key
99 xylem hydraulic traits. Differences in the anatomy and morphology of the conductive xylem cell
100 structure and anatomy (Hacke et al. 2017) lead to differences in maximum conductivity and the
101 water potential at which cavitation starts to occur (Pockman & Sperry, 2000; Sperry 2003).
102 Within the conifers, there are at least three mechanisms that lead to a tradeoff between xylem
103 safety and efficiency. First is the morphology of the xylem conduit. It is widely acknowledged
104 that narrow (or short) tracheid are safer than wider (or longer) tracheid but have lower
105 conductance per sap area (Choat and Pittermann 2009). Second are the intervessel pit
106 membranes. Thicker and less porous membranes prevent the spread of air but increase the
107 hydraulic resistance of xylem (e.g. Li et al., 2016; Pratt & Jacobsen 2017). The third mechanism
108 comes from the division of limited space (Pratt and Jacobsen 2017). With the same cross
109 sectional area of conduits, vessels with a thicker cell wall provide stronger mechanical support,
110 so that the conduits are less likely to collapse when xylem water potential becomes more
111 negative, however this reduces the area that can be used for conduits transporting water. While
112 these physiological constraints require that the tradeoff does exist to some extent, in many
113 studies, this tradeoff appears to be weak, and there are certainly species that have both safe and
114 efficient xylem. Further, there are many other plant traits that can affect the safety, such as wood
115 density (Pratt and Jacobsen 2017), pit anatomy (Sperry & Hacke 2004, Lens et al. 2011), and
116 biochemistry (Gortan et al. 2011). These traits can have large variation among different plant
117 types. The tradeoff will be weakened when grouping plants at a coarse scale, e.g., by biomass,
118 families and/or across a range of geological and climatic region. But when focusing on certain

119 species in a particular region, the tradeoff becomes stronger, as demonstrated by many local
120 studies (e.g. Barnard et al. 2011, Corcuera et al. 2011, Baker et al. 2019). For example, Kilgore et
121 al. (2021) shows that there is a clear safety-efficiency tradeoff across pine trees in a specific
122 location in the western US. Thus, while we acknowledge that there are many exceptions to the
123 xylem safety-efficiency tradeoff, it is a useful framework for examining plant strategies for
124 dealing with drought.

125 The traits that govern the hydraulic function of plant root systems are also critically
126 important, but the least understood, studied, and quantified. These traits include the rooting
127 depth, the root to shoot ratio, the vertical and lateral distribution of roots, and the fine root
128 density and diameter, all of which are related to water uptake (Canadell et al., 2007, Allen
129 2009, Reichstein et al., 2014, Wullschleger et al. 2014). In general, species with deeper roots can
130 access water at greater depths, that is unavailable to more shallowly rooted species (Jackson et
131 al., 1996; Canadell et al., 1996). The vertical root distribution can affect the water uptake and
132 thus the evapotranspiration (ET) pattern during the dry-down period (Teuling, Uijlenhoet, and
133 Troch 2006). This in turn affects the seasonal distribution of water over the soil depth, and
134 thereby the resilience of plants to seasonal droughts (Yu, Zhuang, and Nakayama 2007). The
135 vertical root distribution is also a means of belowground niche differentiation (Ivanov et al.
136 2012; Kulmatiski and Beard 2013), whereas the extent of the lateral root distribution dictates the
137 competition for water (Agee et al. 2021). Whether a plant can benefit from having deep roots
138 is related to the plant's leaf and xylem hydraulic traits (e.g. Johnson et al. 2018, Mackay et al.
139 2020), thus requiring coordination of rooting and hydraulic traits.

140 Given the strength of the Mediterranean-type climate of California, the coordination of
141 rooting and hydraulic strategies will play a critical role for forest dynamics. However, the
142 interplay of rooting and hydraulic strategies and their impact on ecosystem processes haven't
143 been well understood. In this study, we address this question at the Soaproot site (CZ2) of the
144 southern Sierra Nevada of California as the study area. The CZ2 site was strongly affected by the
145 2012-2015 drought, with extremely high tree mortality rates (~90% of the pine died) (Fettig et al.
146 2019). While the 2012 - 2015 drought was widespread across California, the highest rates of tree
147 mortality occurred in the southern Sierra Nevada, centered around an elevation similar to this site
148 (1160 m to 2015 m, Asner et al. 2016, Goulden and Bales 2019). This mid-elevation region is

149 also characterized by the highest forest productivity along an elevation gradient from foothill
150 woodlands to subalpine forest (Kelly and Goulden 2016). This leads us to ask whether strategies
151 associated with high productivity have exposed trees to high mortality risk under prolonged
152 drought.

153 Specifically, here we use the Functionally Assembled Terrestrial Ecosystem Simulator, in
154 a configuration that includes plant hydraulics (FATES-Hydro), to explore the tradeoffs
155 associated with differing hydraulic strategies, and in particular their implications for plant
156 productivity and risk of drought-induced mortality. We conduct a sensitivity analysis, using
157 FATES-Hydro in comparison with observations from the CZ2 eddy covariance site, to
158 investigate how stomatal, xylem and rooting strategies affect the ecosystem and physiologic
159 processes of the forest, and whether that may explain the high rates of both productivity and
160 drought-associated mortality of conifers at CZ2. We note that this is not an exhaustive
161 model parameter sensitivity study. The main purpose is to use a sensitivity analysis to
162 explore scientific questions around hydraulic trait tradeoffs.

163 **2. Methods**

164 2.1 Study site

165 The Soaproot site is a 543-ha headwater catchment at 1100m elevation (37°2.4' N,
166 119°15.42' W), which is at the lower boundary of the rain–snow transition line with warm, dry
167 summers and cool, wet winters (Geen et al. 2018). The mean annual temperature is about 13.8°C
168 (Goulden et al., 2012). Under normal conditions, the annual precipitation is about 1300 mm, but
169 during a dry year, the precipitation can drop to 300-600mm. (Bales et al. 2018). The site is a
170 ponderosa pine (*Pinus ponderosa*) dominated conifer ecosystem exhibiting high productivity
171 (Kelly and Goulden (2016) reported 2.1 tC/ha/year average annual gross stem wood production
172 averaged). Other species include California black oak (*Quercus kelloggii* Newberry), and incense
173 cedar (*Calocedrus decurrens*).

174 Soils at the Soaproot site are mainly of the Holland (fine-loamy, mesic Ultic Haploxeralfs)
175 and Chaix (coarse-loamy, mesic Typic Dystroxerepts) series, which are representative of soils
176 across a similar elevation band of the western Sierra Nevada (Mooney and Zavaleta 2003). Soils
177 of the Holland series have sandy loam surface texture and underlying Bt horizons with sandy

178 clay loam textures, while soils of the Chaix series have sandy loam textures throughout the
179 profile. The regolith depth is estimated to be 15m (Holbrook et al., 2014). The total porosity over
180 the whole regolith depth of the site is estimated to be 1620 mm and the total available storage
181 porosity (plant accessible water storage capacity), which is the difference in volumetric water
182 content between field capacity and permanent wilting point ($\sim -6\text{Mpa}$) to be 1400 mm (Klos et
183 al. 2017). The available water storage capacity is approximately $0.20\text{ cm}^3\text{ cm}^{-3}$ in the upper
184 regolith (0–5 m depth) which decreases to $0.05\text{ cm}^3\text{ cm}^{-3}$ or less in the lower regolith (below 5
185 m depth) (Holbrook et al., 2014).

186 An eddy-covariance flux tower was installed at this site in September 2010. The elevation
187 of the tower is 1160 m above sea level. Instruments on the flux tower track changes in carbon
188 dioxide, water vapor, air temperature, relative humidity, and other atmospheric properties. We
189 compare the simulated gross primary productivity (GPP) and latent heat flux with the flux tower
190 measurements over the period from 2011 to 2015 (Goulden and Bales 2019). We computed the
191 Root Mean Square Error (RMSE) of the hourly mean diurnal cycle of each month. This allows
192 us to examine the capacity of FATES-Hydro to predict the carbon and water fluxes. The
193 transpiration at the site contributed to the majority of the ET as indicated by the measurements
194 from an adjacent catchment, as well as the fact that the site is fully vegetated with an annual LAI
195 around 3 to 4.

196

197 2.2 FATES-Hydro model and parameterization

198 2.2.1 The FATES-Hydro model

199 FATES is a cohort-based, size- and age-structured dynamic vegetation model, where long-
200 term plant growth and mortality rates and plant competition emerge as a consequence of
201 physiological processes. In the model, multiple cohorts grow on the same land unit, share the soil
202 water, and interact with each other through light competition. FATES is coupled within both the
203 CLM5 (Lawrence et al., 2019) and the ELM (Golaz et al., 2020) land surface models (LSMs). In
204 this study, FATES is coupled with the CLM5. FATES-Hydro is a recent development of the
205 FATES model (Fisher et al., 2015; Koven et al., 2020), in which a plant hydro-dynamic module,
206 originally developed by Christoffersen et al. (2016), is coupled to the existing photosynthesis

207 and soil hydraulic modules. FATES-Hydro is described in more detail by Xu et al., (in review,
208 <https://doi.org/10.5194/egusphere-2023-278>) and its supplementary material.

209 Conceptually, plant hydraulic models can be broadly grouped into two types. The first
210 group represents the plant hydraulic system as analogous to an electrical circuit (e.g. Mackay et
211 al. 2011, Huang et al. 2017, Eller et al. 2018, Kennedy et al. 2019). The total resistance of the
212 plant is calculated from the resistance of each compartment using Ohm's law. There is no storage
213 of water in the plants and the transpiration from plants at any given time step is considered to
214 come directly from soil storage. The second group represents plant hydraulics by a series of
215 connected porous media, corresponding to each plant compartment (e.g. Bohrer et al. 2005 ,
216 Janott et al. 2011, Xu et al., 2016, Christoffersen et al., 2016). The porous media model takes
217 into account the water storage in the plant. The flow between two adjacent compartments is
218 driven by the difference in the water potential, mediated by the hydraulic conductivity. FATES-
219 Hydro falls in the second group. The various models in the second group differ in the exact
220 formulas used to describe the pressure-volume and pressure-conductivity relations, as well as
221 different numbers and arrangement of nodes within the soil-plant-atmosphere system.

222 In FATES-Hydro, for each plant cohort, the hydraulic module tracks water flow along a
223 soil-plant-atmosphere continuum of a representative individual tree based on hydraulic laws,
224 and updates the water content and potential of leaves, stem, and roots with a 30 minute model
225 time step. Water flow from each soil layer within the root zone into the plant root system is
226 calculated as a function of the hydraulic conductivity as determined by root biomass and root
227 traits such as specific root length, and the difference in water potential between the absorbing
228 roots and the rhizosphere. The vertical root distribution is based on Zeng's (2001) two parameter
229 power law function which takes into account the regolith depth:

$$230 \quad Y_i = \frac{0.5(e^{-r_a z_{li}} + e^{-r_b z_{li}}) - 0.5(e^{-r_a z_{ui}} + e^{-r_b z_{ui}})}{1 - 0.5(e^{-r_a z} + e^{-r_b z})}, \quad (\text{Eq 1})$$

231 where Y_i is the fraction of fine or coarse roots in the i th soil layer, r_a and r_b are the two
232 parameters that determine the vertical root distribution, Z_{li} is the depth of the lower boundary of
233 the i th soil layer, and Z_{ui} is the depth of the upper boundary of the i th soil layer, and Z is the total

234 regolith depth. The vertical root distribution affects water uptake by the hydrodynamic model by
 235 distributing the total amount of root, and thus root resistance, through the soils.

236 The total transpiration of a tree is the product of total leaf area (LA) and the transpiration
 237 rate per unit leaf area (J). In this version of FATES-Hydro, we adopt the model developed by
 238 Vesala et al. (2017) to take into account the effect of leaf water potential on the within-leaf
 239 relative humidity and transpiration rate:

$$E = LA \cdot J \quad (\text{Eq 2a})$$

$$J = \rho_{atm} \frac{(q_l - q_s)}{1/g_s + r_b} \quad (\text{Eq 2b})$$

$$240 \quad q_l = \exp\left(\frac{w \cdot LWP \cdot V_{H2O}}{R \cdot T}\right) \cdot q_{sat} \quad (\text{Eq 2c})$$

241 where E is the total transpiration of a tree, LA is the total leaf area (m²), J is the transpiration per
 242 unit leaf area (kg s⁻¹ m⁻²), ρ_{atm} is the density of atmospheric air (kg m⁻³), q_l is the within-leaf
 243 specific humidity(kg kg⁻¹), q_s is the atmosphere specific humidity (kg kg⁻¹), g_s is the
 244 stomatal conductance per leaf area, r_b is the leaf boundary layer resistance(s m⁻¹), w is a
 245 scaling coefficient (unitless), which can vary between 1 and 7, and here we use a value of 3;
 246 LWP is the leaf water potential (Mpa), V_{H2O} is the molar volume of water (18×10^{-6} m³ mol⁻¹), R
 247 is the universal gas constant, and T is the leaf temperature (K).

248 The sap flow from absorbing roots to the canopy through each compartment of the tree
 249 along the flow path way (absorbing roots, transport roots, stem, and leaf) is computed
 250 according to Darcy's law in terms of the plant sapwood water conductance, the water potential
 251 gradient:

$$252 \quad Q_i = -K_i [\rho_w g (z_i - z_{i+1}) + (\Psi_i - \Psi_{i+1})] \quad (\text{Eq 3})$$

253 where ρ_w is the density of water; z_i is the height of the compartment(m); z_{i+1} is the height
 254 of the next compartment down the flow path (m); Ψ_i is the water potential of the

255 compartment(Mpa); Ψ_{i+1} is the water potential of the next compartment down the flow
 256 path(Mpa); and K_i is the hydraulic conductivity of the compartment ($\text{kg Mpa}^{-1} \text{ m}^{-1} \text{ s}^{-1}$).
 257 The hydraulic conductivity of the compartments is by the water potential and maximum
 258 hydraulic conductivity of the compartment through the pressure-volume (P-V) curve and the
 259 vulnerability curve (Manzoni et al. 2013, Christoffersen et al. 2016).

260 The plant hydrodynamic representation and numerical solver scheme within FATES-
 261 HYDRO follows Christoffersen et al. (2016). We made a few modifications to accommodate the
 262 multiple soil layers and to improve the numerical stability. First, to accommodate the multiple
 263 soil layers, we have sequentially solved the Richards' equation for each individual soil layer,
 264 with each layer-specific solution proportional to each layer's contribution to the total root-soil
 265 conductance. Second, to improve the numerical stability, we have an option to linearly
 266 extrapolate the PV curve beyond the residual and saturated tissue water content to avoid the rare
 267 cases of overshooting in the numerical scheme under very dry or wet conditions. Third,
 268 Christoffersen et al. (2016) use three phases to describe the PV curves: 1) dehydration phases
 269 representing capillary water (sapwood only), 2) elastic cell drainage (positive turgor), and 3)
 270 continued drainage after cells have lost turgor. Due to the possible discontinuity of the curve
 271 between these three phases, it leads to the potential for numerical instability. To resolve this
 272 instability, FATES-HYDRO added the Van Genuchten model (Van Genuchten 1980, July and
 273 Horton 2004) and the Campbell model (Campbell 1974) as alternatives to describe the PV
 274 curves.

275 In this study, we use the Van Genuchten model because of two advantages: 1) it is simple,
 276 with only three parameters needed for both curves, and 2) it is mechanistically based, with both
 277 the P-V curve and vulnerability curve derived from a pipe model, and thus connected through
 278 three shared parameters:

$$\Psi = \frac{1}{-\alpha} \cdot \left(\frac{1}{Se^{1/m}} - 1 \right)^{1/n} \quad (\text{Eq 4a})$$

$$FMC = \left(1 - \left(\frac{(-\alpha \cdot \Psi)^n}{1 + (-\alpha \cdot \Psi)^n} \right)^m \right)^2 \quad (\text{Eq 4b})$$

279

280 where Ψ is the water potential of the media (xylem in this case) (Mpa); FMC is the fraction of
 281 xylem conductivity, K/K_{max} , (unitless); α is a scaling parameter for air entry point (Mpa⁻¹), Se
 282 is the dimensionless standardized relative water content as $Se=(\theta - \theta_r)/(\theta_{sat} - \theta_r)$ with θ , θ_r , θ_{sat}
 283 are volumetric water content (m³ m⁻³), residual volumetric water content, and saturated
 284 volumetric water content correspondingly; and m and n are dimensionless (xylem conduits) size
 285 distribution parameters. The model assumes that xylem conductance can be restored as xylem
 286 water content increases due to increased water availability after a dry period without any
 287 hysteresis in the FMC curve.

288

289 The stomatal conductance is modelled in the form of the Ball-Berry conductance model
 290 (Ball et al. 1987, Oleson et al. 2013, Fisher et al. 2015):

$$291 \quad g_s = b_{slp} \frac{A_n}{c_s / P_{atm}} \frac{e_s}{e_i} + b_{opt} \beta_t, \quad (\text{Eq 5})$$

292 where b_{slp} and b_{opt} are parameters that represent the slope and intercept in the Ball-Berry model,
 293 correspondingly. These terms are plant strategy dependent and can vary widely with plant
 294 functional types (Medlyn et al. 2011). The parameter b_{opt} is also scaled by the water stress index
 295 β_t . A_n is the net carbon assimilation rate ($\mu\text{mol CO}_2 \text{ m}^{-2} \text{ s}^{-1}$) based on Farquhar's (1980)
 296 formula. This term is also constrained by water stress index β_t in the way that the $V_{cmax,25}$ is
 297 scaled by β_t as $V_{cmax,25}\beta_t$ (Fisher et al. 2018). c_s is the CO₂ partial pressure at the leaf surface
 298 (Pa), e_s is the vapor pressure at the leaf surface (Pa), e_i is the saturation vapor pressure (Pa) inside
 299 the leaf at a given vegetation temperature when $A_n = 0$.

300 The water stress index β_t , a proxy for stomatal closure in response to desiccation, is
 301 determined by the leaf water potential adopted from the FMC_{gs} term from Christoffersen et al.
 302 (2016):

$$\beta_l = \left[1 + \left(\frac{\Psi_l}{P50_{gs}} \right)^{a_{gs}} \right]^{-1} \quad (\text{Eq 6})$$

303

304 where Ψ_l is the leaf water potential (MPa), $P50_{gs}$ is the leaf water potential of 50% stomatal
 305 closure, and a_{gs} governs the steepness of the function. For a given value of a_{gs} , the $P50_{gs}$ controls
 306 the degree of the risk of xylem embolism (Christoffersen et al. 2016, Powell et al. 2017). A more
 307 negative $P50_{gs}$ means that, during leaf dry down from full turgor, the stomatal aperture stays
 308 open and thus allows the transpiration rate to remain high and xylem to dry out, which thus can
 309 maintain high photosynthetic rates, at the risk of exposing xylem to embolism and thus plant
 310 mortality. Conversely, a plant with a less negative $P50_{gs}$ will close its stomata quickly during
 311 leaf dry down, thus limiting transpiration and the risk of xylem embolism and mortality
 312 associated with it, at the cost of reduced photosynthesis.

313

314 2.2.2 Sensitivity analysis and Parameterization

315 The goal of this analysis is to better understand how coordinated aboveground and
 316 belowground hydraulic traits determine plant physiological dynamics and the interplay between
 317 ecosystem fluxes and tissue moisture during the extreme 2012-2015 drought at the Soaproot site.
 318 We thus conduct a global sensitivity analysis on selected hydraulic parameters to explore the
 319 linkages of aboveground and belowground hydraulic strategies. We use a full-factorial design for
 320 the parameter sensitivity analysis in order to best investigate the relationships between
 321 parameters. Because this design requires a relatively small set of parameters or groups of
 322 parameters to vary, we chose parameters that represent the major axes of relatively well-
 323 understood stomatal, xylem and rooting mechanisms/strategies that control the hydraulic
 324 functioning of trees. We set the values of these parameters within the realistic (allowable
 325 biological) range based on online database, and literatures where the species and physical
 326 environment are as close to our system as possible. We list other major parameters and their
 327 estimates that are not varied in the sensitivity analysis (table 2). We acknowledge that the biggest
 328 disadvantage of this study is the lack of sufficient field data to constrain the model. This is a
 329 result of using a natural drought as an experiment of opportunity, which because it was not

330 anticipated, did not allow for as coordinated planning as would be the case in an experimentally-
331 manipulated drought. The trees at that site had all died by the time we started this study.

332 The parameters that we vary here are 1) the pair of r_a and r_b , which control vertical root
333 distribution as deep vs shallow roots, 2) two sets of xylem parameters (P_{50x} , K_{max} , m , n , and α)
334 that jointly represent two distinct xylem strategies: efficient/unsafe and inefficient/safe xylem
335 within the range observed for temperate conifer trees, and 3) the stomatal parameter $P50_{gs}$, which
336 represents the stomatal strategy along a risky to safe gradient (Table 1). The ranges of root
337 parameters are chosen so that the effective rooting depth, above which 95% of root biomass
338 stays, varies from 1m to 8m which is the possible range at the Soaproot site, as indicated by
339 current knowledge of the subsurface structure (see Klos et al., 2017). Note, here we refer to a
340 higher proportion of roots in deep subsurface layers as ‘deep rooting’ (e.g effective rooting depth
341 = 8m; $r_a=0.1, r_b=0.1$) as compared to ‘shallow rooting’ (e.g effective rooting depth = 2; $r_a=1, r_b=5$)
342 which represents a larger proportion of fine roots in upper layers (Figure 1a).

343 The safety-efficiency tradeoff of xylem has been widely discussed in the literature (e.g.
344 Gleason et al. 2016; Hacke et al. 2006, 2017; Martinez-Vilalta, Sala, and Piol 2004). Given that
345 we don’t have any measurements that can be used to generate a vulnerability curve at our study
346 site, we consult the literature (Domec et al. 2004, Barnard et al. 2011, Corcuera et al. 2011,
347 Anderegg and Hillerislambers 2016, Baker et al. 2019, Kilgore et al. 2021) for observed curves
348 from sites that are as similar both in climate (e.g mean annual precipitation and temperature)
349 and in the set of conifer species (*P. Ponderosa*) to our study site as possible, as well as
350 values of xylem traits (K_{max} and $P50_x$) of *Ponderosa* pine in temperate regions of the TRY
351 database (Kattge et al. 2020) to determine the two hypothetical vulnerability curves representing
352 the safe/inefficient and unsafe/efficient xylem strategies. We set the parameters of the van
353 Genuchten model to represent these two sets of P-V and vulnerability curves as shown in
354 Fig1b and 1c. It is worth noting that with the same K_{max} and $P50$, the exact shape of the
355 vulnerability can differ depending on the formula used and parameter values. However,
356 this should not be an issue in our study because the vulnerability curve is mainly constrained
357 by P50 and Kmax. Second, given that there is a large range of variation in the measured
358 values, the effect caused by the exact shape of the curves is minor. Third, since the objective of
359 our study is not to accurately predict mortality, but rather to examine the effect of different

360 combination of stoma, xylem, and root strategies, even if the shape of our vulnerability curve is
361 not the most accurate, as long as the curve captures the overall pattern of the pressure-
362 conductivity relation, it will not affect the relative outcome of this study.

363 We follow the theory of Skelton et al. (2015) to define safe vs. efficient stomatal strategy.
364 In FATES-Hydro, there are two key stomatal parameters: $P50_{gs}$ and a_{gs} . Here, we only vary
365 $P50_{gs}$ while keeping a_{gs} as a constant because the objective here is to choose the parameters that
366 are relatively well understood and to catch the safe vs. risky strategies as described by Skelton et
367 al., rather than to exhaust the parameter space within the model. In essence, the different
368 combinations of $P50_{gs}$ and the shape parameter (a_{gs}) can generate similar stomatal response
369 curves. For example, a small negative $P50_{gs}$ with small a_{gs} would result in a flat stomatal
370 response curve, which is similar to a large negative $P50_{gs}$ combined with a large a_{gs} . Further,
371 $P50_{gs}$ is well understood and has more observed data, while a_{gs} is less studied and barely has any
372 observed data. With a given a_{gs} , the variance of $P50_{gs}$ for a given P_{xylem} value, controls
373 the degree of embolism risk, from a ‘risky’ strategy, where $P50_{gs}$ is equals to or lower than
374 P_{xylem} , to a ‘conservative’ strategy, where $P50_{gs}$ is higher than P_{xylem} . The P_{xylemS} in Skelton et
375 al.’s (2015) are for Fynbos species, therefore are not appropriate for our study because our
376 species are pine trees, a woody plant. Trees have woody tissue which contribute to strengthen the
377 conduits and make them less easy to collapse when embolized, hence allow their stomata to be
378 riskier than herbaceous plants. From the observed $P50_{gs}$ and xylem traits of closely related pine
379 species in the TRY database (Kattge et al. 2020) and elsewhere in the literature (Bartlett et al.
380 2016), as well as the observed soil water potential at the study site, we choose to vary $P50_{gs}$
381 between $P50_{xylem}$ and $P20_{xylem}$, (correspondingly the point at which xylem have lost 50% and
382 20% of their maximum conductivity).

383 The emergent behavior of FATES or any model with dynamic ecosystem structure can
384 make analysis of physiological rate variation difficult, as the stand structure will respond and
385 thus also vary when parameters are changed. Here, we wanted to first understand the direct trait
386 control in the absence of structural differences. To overcome complication of the dynamic
387 structure, we use a reduced complexity configuration for running the model which we refer to as
388 ‘static stand structure’ mode. To investigate dynamic competitive effects when growth and
389 mortality will be the next step. In this mode, the stand structure is initialized from observed

390 forest census data, and subsequently is fixed, i.e. the model does not permit plant growth or death
391 to change the vegetation structure. This allows the direct assessment of hydraulic and
392 physiological parameter variation in the model without the consequent feedback loops associated
393 with varying ecosystem structure. The stand structure is initialized with census data from the
394 CZ2 site (Table S1) and thus includes multiple cohorts of different sized trees. Because this type
395 of model configuration ignores prognostic plant mortality, in the interest of being able to
396 compare across simulations where mortality rates might otherwise be very high, we use the loss
397 of xylem conductivity as a measure of mortality risk of conifer trees at CZ2, which has widely
398 been used as an indicator of drought mortality of forest (e.g. Hammond et al., 2019).

399 To force the model with an atmospheric upper boundary, we use the Multivariate Adaptive
400 Constructed Analogs (MACA) climate data (Abatzoglou and Brown 2012) from 2008 – 2015 of
401 a 4km x 4km grid covers the study area. The daily average MACA data are disaggregated to 3-
402 hourly climate data (see Appendix S2 in Buotte et al. 2018 for detail) . We set the initial soil
403 water content to be 75% of saturated water content, close to field capacity. We believe this is a
404 realistic value because the model is initialized in January, when the study area has high
405 precipitation and trees are all in a dormant status, and in a year when there is not drought. We
406 also tried to initialize the soil with higher water content (e.g. saturation), but did not find any
407 differences, as the extra water drained quickly in the winter when transpiration is low.

408 **3. Results**

409 3.1 Sensitivity of GPP and ET to parameter perturbations

410 The parameter sensitivity analysis shows that in a monthly-mean flux comparison, the
411 simulations with deep roots give a better match to the overall observed pattern of GPP and ET
412 (Fig. 2). The simulated transpiration contributes to 90% of the ET in general. The deep-rooted
413 cases better capture the seasonality (e.g. the peak time) and the declining trend of observed GPP
414 from 2011 to 2015. The deep-rooted cases also match fairly well the observed ET. The simulated
415 GPP of shallow-rooted cases are higher than observed values during wet seasons (Dec. to Mar.),
416 but much lower than the observed values during dry season of the pre-drought period. The
417 simulated ET of shallow-rooted cases are overall lower than the observed values. To quantify
418 this assessment, we computed Root Mean Square Error (RMSE) from the hourly mean GPP and

419 ET of each month each year of all the 40 cases (Fig. S2). We choose RMSE as it is a common
420 and compact metric of assessing model performance, though we note that other metrics could in
421 principle be used, each of which has different advantages and disadvantages (e.g. Collier et al.,
422 2018). The RMSE of GPP and ET decreases with both effective rooting depth and P50gs for
423 both xylem strategies (Fig. 3). The P50gs has less impact on the RMSE of GPP for the case
424 with safe xylem than on that of the case with efficient xylem. In terms of GPP, the effective
425 rooting depth of 6.5m gives the best fit, as indicated by the darkest color (RMSE of GPP =
426 $1.12\text{gC/m}^2/\text{s}$, RMSE of ET = 250 W/m^2), underscoring the importance of deep roots in
427 maintaining transpiration and photosynthesis during the dry season, as well as the role of deep
428 roots in increasing the relative decline in these fluxes during the drought.

429 Among the parameters we varied in the sensitivity analysis, the vertical root distribution
430 has the largest impact on GPP and ET at CZ2. Figures 2a-2b show the monthly mean GPP and
431 ET of the end members of the sensitivity analysis (see Fig. S1 for the complete set of outcomes).
432 We acknowledge that the variation in rooting depth across the ensemble is large, but point out
433 that so is uncertainty in plant rooting depth, and moreover that the uncertainty in rooting depth is
434 less well-quantified than other plant traits such as P50, such that this wide variation reflects a
435 real and deep uncertainty in plant rooting profiles. Deep roots result in substantially higher GPP
436 and transpiration during normal years (2011 and 2012). During long-term droughts, when deep
437 soil moisture is depleted, the relative advantage of deep roots over shallow roots is reduced.
438 Shallow roots result in substantially lower GPP and transpiration during the dry season (Aug. to
439 Oct.), with seasonal maximum occurring earlier, in May, as compared to July with the deep-
440 rooted cases. The shallow-rooted cases also have much lower GPP and ET during the dry
441 seasons of the pre-drought period. During the late stage of drought (2014 and 2015), the GPP and
442 ET of the different cases become more similar between the shallow- and deep-rooted cases.

443 The second set of parameters in importance to rooting depth for controlling carbon and
444 water fluxes is the stomatal strategy. The simulations with a more risky strategy ($P50_{gs}=P50_x$)
445 gives higher GPP and ET than the simulations with a safer strategy ($P50_{gs}=P20_x$) during pre-
446 drought periods and the early stage of the drought (2011 to 2013), but slightly lower GPP and ET
447 at the late stage of the drought (2014 and 2015) for the deep-rooted cases. However, risky
448 stomata gives slightly higher GPP and ET at all times for shallow-rooted cases. The xylem

449 strategy has the smallest effect on GPP and ET of the parameters we varied (e.g., RMSEs of ET
450 are both around 260 W/m^2 for safe and efficient xylem, respectively, with $P50gs = P20x$ and 8m
451 effective rooting depth). In deep-rooted cases, the safe xylem and efficient xylem strategy result
452 in almost the same GPP and ET, which can be seen via the wide overlap between the dashed
453 and solid lines in figure 1. In shallow-rooted cases, with safe stomata, safe xylem generates
454 slightly higher GPP and ET than efficient xylem. In addition, the strength of effects of
455 stomatal and xylem strategy also depend on the rooting depth. The deeper the effective rooting
456 depth, the less significant the impacts of stomatal strategy (Fig. S1).

457

458 3.2 Sensitivity of plant water status to parameter perturbations

459 We examine the impact of vertical root distributions, stomatal and xylem strategies on the
460 seasonal variation of three plant physiologic variables that serve as indices of plant water stress
461 (fig. 4): the fraction loss of xylem conductivity of stem (SFL), leaf water potential (LWP), and
462 an overall absorbing root water potential (AWP). In the model, absorbing roots in different
463 soil layers have different water potentials, associated with the soil water potential of that layer.
464 We calculate a cohort-level effective AWP as the root-fraction-weighted average of water
465 potential in absorbing root across all soil layers. In this way, the AWP represents the overall
466 rhizosphere soil moisture condition that is sensed by the tree. These physiological variables are
467 tracked for each cohort. For any given case, the differences in these variables among differently-
468 sized cohorts are negligible (Fig. S3). Therefore, we present the outcome of all cohorts with
469 a diameter at breast height (DBH) between 50 – 60cm, the size class that is most abundant at
470 CZ2.

471 Stomatal and rooting strategies together control the loss of xylem conductivity during the
472 dry season of the pre-drought period and the whole period of the long-term drought (Fig 4a). In
473 all cases, the xylem conductivity reaches a maximum during the wet season (Dec. to Jan.), starts
474 to decline during the growing season (Apr. to Jun.), then reaches its minimum in the dry season.
475 With the same stomatal strategy, deep roots lead to less-extreme loss of xylem conductivity than
476 shallow roots. A deep rooting strategy is also able to maintain xylem conductivity with very
477 little seasonal loss during the pre-drought period, but as deep soil moisture is depleted, this effect
478 is reduced. With a shallow rooting profile, the xylem conductivity starts to decline earlier and the

479 minimum is much lower than that of a deep rooting profile. For example, with risky stomata, the
480 minimum fraction of xylem conductivity of deep-rooted cases in 2012 is 0.4, but is lower than
481 0.2 with shallow roots. Unlike deep-rooted cases, in shallow-rooted cases, the seasonal variation
482 of the loss of xylem conductivity does not differ too much during pre-drought and drought
483 periods. During the very late stage of the drought, deep-rooted cases have a lower fraction of
484 xylem conductivity than shallow-rooted cases (e.g., in Jan. 2015).

485 In general, risky stomata allow a greater loss of xylem conductivity (K/K_{max}) than safe
486 stomata, but the extent depends on the vertical root distribution. The effect of the stomatal
487 strategy is more obvious in shallow-rooted cases. Risky stomata combined with shallow roots
488 result in increasing the duration of 50% loss of xylem conductivity, as well as the maximum
489 loss of xylem conductivity during the dry season. With a deep rooting strategy, the difference in
490 the percentage loss of xylem conductivity between safe stomatal and risky stomatal cases
491 increases with the progression of the drought, but with a shallow rooting strategy, this difference
492 remains more or less the same over time. In addition, in 2011, a very wet year, with deep roots, a
493 safe xylem strategy is able to maintain the maximum xylem conductivity even during dry season
494 (Fig 4a). The impact of xylem strategy on the percentage loss of xylem conductivity is relatively
495 weak. For both deep- and shallow-rooted cases, trees with safe xylem lose less xylem
496 conductivity during the wet season but lose more conductivity during the dry season.

497 The safe stomata & safe xylem cases for both deep- and shallow-rooted trees experience
498 greater declines in stem conductivity as compared to the safe stomata and efficient xylem for the
499 corresponding rooting depths (Fig. 4a). This is because with safe stomata, trees operate at the
500 right end of the vulnerability curve shown in fig. 1b, where the hydraulic conductivity of
501 efficient xylem is much higher than that of the safe xylem. Thus, when transpiring the same
502 amount of water, the efficient xylem will lose less water potential as compared to safe xylem.
503 This keeps the xylem water potential of a plant with efficient xylem higher than one with safe
504 xylem, and consequently also keeps the xylem conductivity, K , higher. This is also because we
505 set $P50_{gs}$ based on P_{xylem} , thus the $P50_{gs}$ of safe stomata for plants with efficient xylem is higher
506 (less negative) than that of plants with safe xylem, thus resulting in lower transpiration rates,
507 which in term reduces the loss of xylem water potential. As a result, plants with both safe
508 stomata and efficient xylem not only transpire less water but also lose less water potential per

509 volume of water transpired. Together, these two mechanisms contribute to keep the xylem
510 conductivity of the efficient xylem cases higher.

511 Stomatal, rooting, and xylem strategies have similar impacts on the seasonal variation of
512 both leaf and fine root water potentials (Fig4c and 4d). Leaf and fine root water potentials peak
513 during the winter, then start to decline in early spring, and reach their lowest point in the dry
514 season. Deep roots, safe stomata, and safe xylem traits all contribute to the maintenance of
515 higher leaf and fine root water potentials during the growing and dry seasons. With deep roots,
516 there is less difference in leaf and fine root water potential between stomatal and xylem
517 strategies in the very wet year 2011. Plants that combine safe stomata and/or safe xylem with
518 deep roots can keep the leaf and fine root water potentials relatively high (less than -5 Mpa)
519 during the dry season of the drought period. However, while plants that combine risky stomata or
520 efficient xylem with deep roots can keep the dry season leaf water potential above -5 Mpa during
521 the pre-drought period, their traits lead to the dry season leaf water potential dropping below -8
522 Mpa or even below -10 Mpa during the drought period. In both deep-rooted and shallow-rooted
523 cases, safe xylem leads to much lower leaf and fine root water potentials during the dry season.
524 The seasonal and inter-annual variation of fine root water potentials are almost identical to the
525 leaf water potential, except that the water potential of fine roots is slightly higher (~ 0.5 Mpa)
526 than the leaf water potential.

527

528 3.3 Sensitivity of subsurface hydrology to parameter perturbations

529 In the simulation outcomes, the vertical root distributions again have the largest impact on
530 hydrologic processes and subsurface water content and the way that they change over the
531 drought. With deep roots, there is less drainage loss from surface and subsurface runoff as
532 compared to shallow roots, especially during the growing season (Figure 5a,c,e,g). The
533 subsurface water content shows different vertical and temporal patterns between the cases with
534 different vertical root distributions. In the deep-rooted cases, during the pre-drought period, the
535 water content in the deepest layers fluctuates between wet and dry seasonally; during the first
536 year of the drought, the water content of the deepest layers (6 to 8m) slightly increases during the
537 wet season, but with the progression of the drought, the soil water content becomes consistently
538 depleted in the middle and deep layers (between 5 and 8 m depth) and only the shallow layer

539 (<0.16 m) water content increases during wet season. In the shallow-rooted cases (Figure
540 5b,d,f,h), soil moisture in the surface layers (top 2m) shows seasonal variation, but this seasonal
541 variation becomes weaker over depth and the soil moisture at 6-8m depth stays consistently high
542 throughout the year during pre-drought period, and remains slightly low through the entire
543 drought period; while the water content of the middle and upper layers of the shallow-rooted
544 case have a similar pattern of seasonal variation before and during the drought.

545 Stomatal strategy, as quantified by $P50_{gs}$, has a weak impact on hydrologic processes and
546 soil moisture. In both the deep- and shallow-rooted cases, riskier stomata lead to a slightly lower
547 total subsurface water content (Figure 6a). The effect of $P50_{gs}$ is less significant during the pre-
548 drought period for both the deep-rooted and shallow-rooted cases, and becomes more significant
549 as the drought progresses. The effect of $P50_{gs}$ on total subsurface water content is less significant
550 in shallow-rooted cases. Figure 5c shows the effect of $P50_{gs}$ on the water content of shallow and
551 deep soil layers. In both the shallow- and deep-rooted cases, increasing $P50_{gs}$ has a negligible
552 impact on the water content of the shallow layers during both the pre-drought and drought
553 periods (Figure 5c left). For deeper layers, in the shallow-rooted case, $P50_{gs}$ has no impact on the
554 water content at all times; in the deep-rooted cases, a risky $P50_{gs}$ results in lower dry season
555 water content of deep layers (7-8m) during the pre-drought period (indicated by the red cycles of
556 Figure 5a and 5c), but decreases the water content of those layers year round during the drought
557 period (Figure 5a and 5e). In deep-rooted cases, safe stomata with efficient xylem lead to a
558 slightly higher water content in deep layers (5m to 8m) during the pre-drought period, and in
559 shallow layers (0 to 3m) during the drought period (Figure 6a). Risky stomata with safe xylem in
560 deep-rooted cases are most effective in accessing soil water. Though the soil water contents are
561 generally high in shallow-rooted cases, stomatal and xylem strategies show a similar impact on
562 the soil water storage as those in the deep-rooted cases (Fig S4).

563 Simulations with deep roots have almost no loss of soil water to drainage during the dry
564 season in normal years, or during the whole drought period; while with shallow roots, the
565 drainage loss is high during the pre-drought period and decreases through the drought period, but
566 still with some runoff even at the end of the drought period (Figure 6a). The observed total
567 annual runoff from the 2008 to 2011 pre-drought period was about 250 mm/year, but was zero
568 during the 2012 – 2015 drought period (from figure 4, Bales et al. 2018). This observed

569 difference in runoff between the pre-drought (~290mm/year, 2011 - 2012) and drought periods
570 (~0 mm/year) from the deep-rooted case is consistent with the predicted pattern. During the pre-
571 drought period, the wet season total subsurface water contents from Dec. to Feb. are similar
572 between the cases with deep and shallow roots, but during the dry season (from June to Sep.) the
573 total subsurface water content with shallow roots is substantially higher than the case with deep
574 roots (Figure 6b).

575 **4. Discussion**

576 4.1 Vertical root distribution as the first order control

577 The outcome of our simulations indicates that the vertical root distribution exerts the first
578 order control over both ecosystem level fluxes and plant physiology at CZ2. This dominance of
579 rooting strategy over other hydraulic traits is related to the nature of the rainfall pattern of the
580 Mediterranean-type climate of that region. The CZ2 site receives effectively all of its rain during
581 winter. This water is stored in the soil column and slowly released through the growing season.
582 The root zone soil moisture has strong seasonal variation, which constrains plant water use and
583 gas exchange as a function of the gradual drying of the soil column (Bales et al., 2018). In the
584 model, the stomatal behavior is controlled by the leaf water potential, which itself is strongly
585 affected by the root zone soil moisture. In our simulations, the daytime average leaf water
586 potential of a 55cm DBH cohort is well correlated with the fine root water potential and is
587 always about 0.5 Mpa lower (fig S5). This offset is consistent with the relationship between mid-
588 day leaf water potential and pre-dawn leaf water potential found by Martínez-Vilalta et al. (2014)
589 at the global scale.

590 With deep roots, trees use more subsurface storage capacity at the CZ2 site, and thus a
591 higher amount of total rainfall. In a wet year such as 2011, the root zone water potential of deep-
592 rooted trees is kept relatively high (Figure 4b) and the trees operate at the upper end of their
593 vulnerability curve through the year, with typical loss of conductivity < 10% (Fig 7). Therefore,
594 we don't see much effect of the stomatal strategy on GPP and transpiration in a wet year. At the
595 upper end of the vulnerability curve, stomata are fully open regardless of the stomatal strategy
596 (either to be safe or risky). When the drought began in late 2012, annual rainfall fell below the
597 total root zone storage, thus the deep storage remained depleted throughout the year. During the

598 drought, the deep-rooted trees were able to operate at the high end of the vulnerability curve in
599 the wet season, when the rainfall recharged the surface layer. As the surface layers dry, water
600 potential then gradually falls to the lower end of the vulnerability curve; consequently the
601 photosynthesis and transpiration start to drop as the dry season progresses. With risky stomata,
602 trees can drive the soil moisture to lower values . This is why we see the difference in the
603 effect on GPP and transpiration between different stomatal strategies during the dry season when
604 the drought progresses.

605 With shallow roots, trees can only use surface soil moisture storage. As a result, the
606 surface water storage is quickly used up after the wet season, and the root zone water potential
607 drops near the low end of the vulnerability curve during the dry season. Thus, the shallow-rooted
608 trees operate along the full extent of the vulnerability curve year-round, both during the pre-
609 drought and drought periods. Therefore, as for the deep-rooted cases, we don't see a strong effect
610 of stomatal strategy on GPP and transpiration during the wet season, but unlike the deep root
611 cases, the effect of stomatal strategy on GPP and transpiration during the dry season can be seen
612 throughout the whole simulation period.

613 Rooting strategies greatly control the spatial pattern of vertical soil water content (Figure
614 5). With deep roots, the vertical soil moisture variation is more homogeneous due to the
615 extensive root distribution. With shallow roots, the soil becomes extremely dry at the surface
616 (<1m) and extremely wet in deep layers (>5m) resulting from the aggregated root distribution in
617 the upper layers. Our finding is similar to a recent study conducted by Agee et al. (2021),
618 where the authors found that the extensive lateral root spreading results in homogeneous soil
619 moisture distribution. The homogeneous soil moisture pattern may contribute to a more energy
620 efficient system that reduces plant water stress (Agee et al. 2021) because that minimizes the
621 energy dissipation loss through water transport (Hildebrandt et al. 2016). Both Agee et al (2021)
622 and our studies emphasize the importance of the means by which the root distributions determine
623 how the subsurface storage is utilized.

624 Given the shape of the vulnerability curves, in all these simulations, plants will stop
625 transpiring when their leaf water potential reaches around -10Mpa with efficient xylem or -
626 15Mpa with safe xylem, depending on their stomatal strategy (Fig 7). Because we are here
627 holding the stand structure and leaf area constant to allow comparison between cases, the

628 simulated leaf water potential of the shallow rooted, risky stomata combination can get as low as
629 -15Mpa (Figure 4b) during dry seasons even during pre-drought period, which is well below the
630 lowest possible leaf water potential observed (-10Mpa) (Vesala et al., 2017). Leaves will likely
631 be wilted before the water potential drops below -10Mpa and the tree would have already shed
632 the leaves due to canopy desiccation. But we specifically do not permit that to occur in these
633 simulations, so as to keep the different cases comparable. Although it might be unrealistic, the
634 leaf water potential can serve as an indicator of the degree of canopy desiccation. With no or
635 very little leaves, trees would rely on the storage carbon to support respiratory demand until
636 the wet season comes to regrow leaves. Depending on the duration of the dry season, trees
637 may exhaust the stored carbon and die from carbon starvation. Risky stomata can generate
638 higher GPP (Figure 1a), but also result in longer duration of more negative leaf water potential
639 (Figure 4b). This suggests that shallow rooted pines at CZ2 with risky stomata will benefit from
640 allocating more net primary productivity to their storage pools rather than growth in order to
641 reduce the carbon-starvation mortality. Therefore, even though the model generates
642 unrealistically low leaf water potentials, the extent and the duration of the simulated very low
643 leaf water potential allows us to gain some insight on the interaction of plant hydraulic strategy
644 and the life history strategy of conifer trees under a Mediterranean-type climate. Further, the
645 unrealistic leaf water potential from the shallow root simulations indicates that the trees at that
646 site must have really deep roots to exist at this site, which is in agreement with the conclusions
647 of Goulden and Bales (2019).

648 In this simulation, the impacts of xylem traits on GPP and ET are weak and subtle. This is
649 the result of the relative position of the two vulnerability curves, in particular, the intersection of
650 the two vulnerability curves in absolute conductivity. When the absolute conductivity is plotted
651 as a function of pressure (fig. 1b and solid lines in fig. S6), it can be seen that, on the left side of
652 the intersection, the safe xylem is not only safe but also efficient, and a safety-efficiency tradeoff
653 of xylem thus only occurs on the right side of the intersection point. Therefore, in shallow-rooted
654 cases, when the root zone water content—and hence plant water status—is low, safe xylem can
655 generate slightly higher GPP and ET than unsafe xylem. Furthermore, the two pressure-
656 conductivity curves diverge mainly at the wet end (corresponding to the wet season). This is
657 likely because the xylem structures of conifers are very similar, and the range of variation of
658 xylem traits in the sensitivity analysis are limited to the dominant species at the site. Therefore,

659 the difference in the xylem traits of conifers do not cause significant impacts on the ecosystem
660 level fluxes under the Mediterranean-type climate of CZ2, where the ecosystem fluxes are
661 constrained by energy during the wet season (Goulden et al., 2012). In addition, the maximum
662 rate of GPP and ET are co-constrained by the stand density, the total leaf area, the maximum
663 stomatal conductance, and VPD. In this study, we used the static stand structure mode of
664 FATES-Hydro, whereby the stand density and the total leaf biomass (so as total leaf area) of the
665 trees are held constant. This further limits the effect of xylem traits on GPP and ET.

666

667 4.2 Balancing productivity and mortality risk

668 The hydraulic traits that contribute to high carbon fixation rates often make trees more
669 susceptible to drought. Stomatal strategy ($P50_{gs}$) can have both positive and negative impact on
670 the trees, creating a tradeoff in the balance between productivity and physiological stress. The
671 risky stomata ($P50_{gs} = P50_x$) can generate higher GPP but also result in a greater loss of xylem
672 conductivity and lower leaf water potential. The tradeoff varies depending on the plant's root
673 strategy—i.e. having a deep vs. a shallow root distribution—and the moisture state.

674 To better understand the tradeoff between productivity and mortality risk, we plot the
675 simulated annual average GPP for each year against the fraction of conductivity (K/K_{max}) of a
676 55cm DBH cohort for two scenarios: deep roots (Fig. 8a) and shallow roots (Fig. 8b), with
677 different combination of xylem and stomatal strategies. In both scenarios, for each pair of xylem
678 and stomatal strategies, the GPP per tree increases almost linearly with the K/K_{max} . But, with
679 increasing the safety of the stomata, the GPP declines faster with loss of conductivity. This
680 response is stronger in deep-rooted scenarios. Having efficient xylem only slightly increases
681 the steepness of the lines. The stomatal strategies thus represent points along a gradient of the
682 tradeoff between growth and mortality risk - the safer the stomata, the more GPP is traded for
683 reducing the mortality risk.

684 Along this tradeoff space, where trees can maximize their net carbon gains likely depends
685 on the xylem traits. Studies have shown that trees may temporarily lose xylem conductivity
686 during mild drought, which can recover once the soil water becomes available. However, under
687 an extreme drought, their xylem could collapse and permanently damage the xylem conduits. In

688 this case, trees rely on new sapwood growth to support the transpiration (Brodrribb et al. 2010,
689 Anderegg et al. 2013). At one extreme, if the stomatal behavior is too safe, it will give low GPP
690 and the tree will be outcompeted for light due to faster-growing neighbors, but at the other
691 extreme, if the stomata behave very aggressive (risky), it will give high GPP but also empty the
692 subsurface storage quickly, consequently leading to a prolonged dry period of soil moisture. This
693 would lead to substantial xylem damage (and/or root death), and then the carbon needed to grow
694 new sapwood (or roots) can exceed the benefit of getting the additional GPP. So, the optimal
695 location along the gradient would probably be located slightly below the K/K_{max} associated
696 with that critical xylem water potential. Currently, the xylem refilling and associated carbon cost
697 are not incorporated in FATES-Hydro. These two processes should be implemented in the
698 model to better understand the water-carbon balance, and thus remains as future work.

699 In the deep-rooted scenario, the values of the pre-drought period and early drought stage
700 are clustered at the upper-right corner, above K/K_{max} of 0.6. (Fig. 8a). In this region, the stress
701 from the loss of xylem conductivity likely won't be high enough to cause severe consequences, if
702 using 50 percent loss of xylem conductivity as the threshold for mortality and/or permanent
703 xylem damage. The deep-rooted tree can thus benefit by trading less GPP for maintaining xylem
704 conductivity with a risky/more-productive stomatal strategy during normal years. But, during the
705 late stage of the drought (2014 and 2015), the conductivity values become much lower. If this
706 mega drought stopped earlier, e.g. if it were a mild drought that only lasted for two years, the
707 additional GPP obtained from risky stomata may outweigh the carbon cost for repairing xylem
708 damage. This suggests that, if the 2012 – 2015 drought was not common in California, natural
709 selection might favor the risky/more-productive stomatal strategy for deep-rooted trees.
710 However, this same strategy also exposes trees to high mortality risk under severe droughts.

711 In the shallow-rooted case (Fig. 8b), the values are all clustered lower and to the left, as
712 compared to deep rooted scenario, irrespective of the drought status. Thus, for shallow roots,
713 risky/more-productive stomatal behavior results in a similarly high mortality risk during both the
714 pre-drought and drought period. Thus, under the long-term climate conditions seen at CZ2,
715 whether or not severe droughts were frequent, the only shallow-rooted trees that could persist
716 would have to follow the safe and less-productive stomatal strategy. And, thus safe and less-
717 productive stomata also protects the shallow-rooted tree plant from mortality risk during drought.

718 The model outcome indicates that under drier root zone soil conditions, if pines were to
719 follow a shallow rooting strategy, they would benefit from a safer stomatal strategy, with more
720 conservative water use; but if they follow a deep rooting strategy, pines would benefit from
721 riskier stomata. This is consistent with Anderegg et al.'s (2016) finding on the relative stomatal
722 conductance (gs) across elevation. They found that at low elevation (lower precipitation) site,
723 Ponderosa pine has lower relative stomatal conductance and less loss of xylem conductivity,
724 equivalent to safer stomata in our study, while at mid elevation (higher precipitation) site, pine
725 has higher relative stomatal conductance and greater loss of xylem conductivity, equivalent
726 to risky stomata in our study. The simulation results are consistent with the idea that the CZ2
727 region is dominated by deep-rooted trees. This is supported by previous studies. In situ
728 measurements of regolith structure (particularly the porosity) indicates that at CZ2, there is a
729 layer of thick semi-weathered bed rock that allows the trees to grow deep roots (Holbrook et
730 al., 2014). Growing deep roots to access rock moisture to support plant water use has also been
731 observed in the Eel River CZO catchment (Rempe et al., 2018), another Mediterranean-type
732 ecosystem along the west coast. Observed net CO₂ exchange and ET during the pre-drought
733 period suggest that during a wet year, deep moisture supported summer transpiration and
734 productivity when the upper layer moisture was low (Goulden et al. 2015). Because the deep
735 rooting strategy is sufficient in most cases to avoid the main effects of dry seasons and short
736 droughts, and that, conditional on having deep roots, the risky stomatal strategy confers a
737 productivity advantage at little increased risk of vulnerability, then we would expect that plants
738 with these traits would dominate. However, under extreme cases such as the 2012 - 2015
739 drought, which ranked as one of the most severe in California in the last 1200 years (Lu et al.
740 2019), we would expect that plants with this deep-rooted, risky stomatal strategy would be
741 highly vulnerable to drought, which is consistent with the ~90% mortality of the pine observed at
742 CZ2 during the drought (Fettig et al. 2019). The water balance of the catchment based on the
743 long-term observation from precipitation, stream flow, and ET (Bales et al. 2018, Goulden and
744 Bales 2019) also support that it was the slow depletion of deep moisture that caused tree
745 mortality in the late stage of the prolonged 2012 – 2015 drought.

746 The finding of our study indicates that the future drought mortality would likely occur in
747 the ecosystems which are co-limited by water and other factors. In those ecosystems, trees can
748 benefit from having more efficient but less safe hydraulic traits, which allow them to be more

749 competitive for water, and bring in higher GPP. The extra carbon gain can be used to develop
750 measures to deal with other constraining factors, such as increase storage carbon to lower the risk
751 of carbon starvation, or build thicker bark to resist fire, and to grow more roots which further
752 enhance their capacity to compete for water.

753 **5. Conclusions**

754 Our analysis indicates that root distribution can affect the most competitive stomatal
755 traits. In a Mediterranean-type climate where the supply of energy and water is
756 desynchronized and accessible subsurface water storage capacity is close to annual precipitation,
757 deep roots combined with risky stomata represent a beneficial strategy for high productivity in
758 normal years with low mortality risk, but exposes trees to high mortality risk during multi-year
759 droughts. While such a strategy enables trees to fully utilize subsurface storage and precipitation
760 for productivity over the regular years, the lack of deep water storage recharge during droughts
761 exposes trees to high drought stress and makes this strategy unfavorable under severe and
762 prolonged drought. In contrast, shallow roots combined with safe stomata represent a strategy for
763 drought resistance, albeit at the cost of considerably reduced productivity, as such a combination
764 only allows trees to use shallow subsurface storage while leaving deep moisture untouched, thus
765 less precipitation is used for productivity. But this strategy leaves trees to be less susceptible to
766 drought-induced mortality should the deep reservoir be depleted. In contrast, shallow roots
767 with risky stomata leads to high mortality even during non-drought years, thus an uncompetitive
768 combination at the site. These results suggest that stomatal strategy is controlled by root zone
769 soil moisture and regulated by root distribution in that region. Thus, our study underscores the
770 importance of considering plant rooting and hydraulic strategies within the larger context of
771 plant ecological strategies.

772

773 **Author contribution**

774 JD and CDK design the study and write the MS. JD conducted the simulation. PB, RB, MG
775 provided model input data. BC, CDK, RF, RK, CX, and JD wrote the code. PB, RB, BC, RF,
776 MG, RK, LK, JS, CX edited the MS.

777

778 **Acknowledgement**

779 We acknowledge support by the Director, Office of Science, Office of Biological and
780 Environmental Research of the U. S. Department of Energy under Contract DE-AC02-
781 05CH11231 through the Early Career Research Program, the University of California Laboratory
782 Fees Research Program, and National Science Foundation Southern Sierra Critical Zone
783 Observatory grant EAR-1331931. RF acknowledges funding by the European Union’s Horizon
784 2020 (H2020) research and innovation program under Grant Agreement No. 101003536
785 (ESM2025 – Earth System Models for the Future) and 821003 (4C, Climate-Carbon Interactions
786 in the Coming Century)

787 **Data availability statement**

788 The FATES code (branch FATEScodeforMS1), parameter files and data that support the
789 findings of this study are openly available at ZENODO:
790 [https://zenodo.org/account/settings/github/repository/JunyanDing/Rooting-and-Hydraulic-](https://zenodo.org/account/settings/github/repository/JunyanDing/Rooting-and-Hydraulic-strategy-of-pine-at-Sierra-CZ2-)
791 [strategy-of-pine-at-Sierra-CZ2-](https://zenodo.org/account/settings/github/repository/JunyanDing/Rooting-and-Hydraulic-strategy-of-pine-at-Sierra-CZ2-) (DOI 10.5281/zenodo.5504405). The flux tower data can be
792 retrieved from the UC Merced online database (<https://www.ess.uci.edu/~california/>).

793 **Competing interests**

794 The authors declare no conflict of interest

795 5. References

- 796 Abatzoglou J.T. and Brown T.J. “A comparison of statistical downscaling methods suited for
797 wildfire applications” *International Journal of Climatology* (2012), 32, 772-780. 2012.
- 798 Adams, H. D. et al. “Mechanisms in Drought-Induced Tree Mortality.” *Nature Ecology &*
799 *Evolution* 1(September). <http://dx.doi.org/10.1038/s41559-017-0248-x>. 2017.
- 800 Agee, E., He, L., Bisht, G., Couvreur, V., Shahbaz, P., Meunier, F. et al., 2021. Root lateral
801 interactions drive water uptake patterns under water limitation. *Adv. Water Resour.*, 151:
802 103896.
- 803 Anderegg, W.R., Plavcová, L., Anderegg, L.D., Hacke, U.G., Berry, J.A. and Field, C.B.,
804 Drought's legacy: multiyear hydraulic deterioration underlies widespread aspen forest die-
805 off and portends increased future risk. *Global change biology*, 19(4), pp.1188-1196. 2013.
- 806 Anderegg, L. D. L. and Hillerislambers, J. Drought stress limits the geographic ranges of two
807 tree species via different physiological mechanisms *Glob. Chang. Biol.* 22 1029–45
808 Online: <http://dx.doi.org/10.1111/gcb.13148> . 2016
- 809 Ando, Eigo, and Kinoshita, Toshinori. “Red Light-Induced Phosphorylation of Plasma
810 Membrane H⁺ -ATPase in Stomatal Guard Cells.” *Plant Physiology* 178(October): 838–49.
811 2018.
- 812 Baker, Kathryn V., Tai, Xiaonan, Miller, Megan L, Johnson, D. M., Six co-occurring conifer
813 species in northern Idaho exhibit a continuum of hydraulic strategies during an extreme
814 drought year, *AoB PLANTS*, Volume 11, Issue 5, October 2019, plz056,
- 815 Bales, Roger et al. “Spatially Distributed Water-Balance and Meteorological Data from the Rain
816 – Snow Transition , Southern Sierra Nevada , California.” : 1795–1805. 2018.
- 817 Bales, Roger et al. 2018. “Mechanisms Controlling the Impact of Multi-Year Drought on
818 Mountain Hydrology.” *Scientific Reports* (December 2017): 1–8.
- 819 Ball, J. Timothy, Ian E. Woodrow, and Joseph A. Berry. "A model predicting stomatal
820 conductance and its contribution to the control of photosynthesis under different
821 environmental conditions." *Progress in photosynthesis research*. Springer, Dordrecht, 221-
822 224. 1987.
- 823 Barnard, DM, Meinzer, FC, Lachenbruch, B., McCulloh, KA, Johnson, DM, Woodruff, D.R.
824 Climate-related trends in sapwood biophysical properties in two conifers: avoidance of
825 hydraulic dysfunction through coordinated adjustments in xylem efficiency, safety and
826 capacitance. *Plant Cell Environ.* Apr;34(4):643-54. doi: 10.1111/j.1365-3040.2010.02269.x.
827 Epub 2011 Feb 11. PMID: 21309793. 2011
- 828 Bartlett, M.K., Klein, T., Jansen, S., Choat, B. and Sack, L., The correlations and sequence of
829 plant stomatal, hydraulic, and wilting responses to drought. *Proceedings of the National*
830 *Academy of Sciences*, 113(46), pp.13098-13103. 2016.
- 831 Brodribb, T.J., Bowman, D.J., Nichols, S., Delzon, S. and Burtlett, R., 2010. Xylem function and
832 growth rate interact to determine recovery rates after exposure to extreme water deficit.
833 *New Phytologist*, 188(2), pp.533-542.

- 834 Buotte, Polly C., Samuel Levis, Beverly E. Law, Tara W. Hudiburg, David E. Rupp, and Jeffery
835 J. Kent. “Near - Future Forest Vulnerability to Drought and Fire Varies across the Western
836 United States.” (July):1–14. 2018.
- 837 Canadell, J.G., Le Quéré, C., Raupach, M.R., Field, C.B., Buitenhuis, E.T., Ciais, P., Conway,
838 T.J., Gillett, N.P., Houghton, R.A. and Marland, G., Contributions to accelerating
839 atmospheric CO₂ growth from economic activity, carbon intensity, and efficiency of natural
840 sinks. *Proceedings of the national academy of sciences*, 104(47), pp.18866-18870. 2007.
- 841 Choat, Brendan, and Jarmila Pittermann. “New Insights into Bordered Pit Structure and
842 Cavitation Resistance in Angiosperms and Conifers.” *New Phytologist*: 555–57. 2009.
- 843 Christoffersen, B. O. et al. “Linking Hydraulic Traits to Tropical Forest Function in a Size-
844 Structured and Trait-Driven Model (TFS v . 1-Hydro).” : 4227–55. 2016.
- 845 Coley, P.D., Bryant, J.P. and Chapin, F.S., Resource availability and plant antiherbivore
846 defense. *Science*, 230(4728), pp.895-899. 1985.
- 847 Corcuera, L., Cochard, H., Gil-Pelegrin, E. and Notivol, E., Phenotypic plasticity in mesic
848 populations of *Pinus pinaster* improves resistance to xylem embolism (P 50) under severe
849 drought. *Trees*, 25(6), pp.1033-1042. 2011.
- 850 Craine, J.M., Tilman, D., Wedin, D., Reich, P., Tjoelker, M. and Knops, J., Functional traits,
851 productivity and effects on nitrogen cycling of 33 grassland species. *Functional*
852 *Ecology*, 16(5), pp.563-574. 2002.
- 853 Danabasoglu, G. et al. “The Community Earth System Model Version 2 (CESM2) Journal of
854 Advances in Modeling Earth Systems.” *Journal of Advances in Modeling Earth Systems* 2:
855 1–35. 2020.
- 856 Domec, J.C., Warren, J.M., Meinzer, F.C. *et al.* Native root xylem embolism and stomatal closure
857 in stands of Douglas-fir and ponderosa pine: mitigation by hydraulic
858 redistribution. *Oecologia* 141, 7–16 <https://doi.org/10.1007/s00442-004-1621-4>. 2004.
- 859 Fettig, Christopher J, Leif A Mortenson, M Bu, and Patra B Fou. “Tree Mortality Following
860 Drought in the Central and Southern Sierra Nevada, California, U.S.” *Forest Ecology and*
861 *Management* 432: 164–78. 2019.
- 862 Fisher, R. a. et al. “Taking off the Training Wheels: The Properties of a Dynamic Vegetation
863 Model without Climate Envelopes, CLM4.5(ED).” *Geoscientific Model Development* 8(11):
864 3593–3619. 2015.
- 865 Gaylord, M.L., Kolb, T.E. and McDowell, N.G.,. Mechanisms of piñon pine mortality after
866 severe drought: a retrospective study of mature trees. *Tree physiology*, 35(8), pp.806-816.
867 2015
- 868 Geen, Anthony Toby O et al. “Southern Sierra Critical Zone Observatory and Kings River
869 Experimental Watersheds : A Synthesis of Measurements , New Insights , and Future
870 Directions.” *Vadose Zone J. Advancing Critical Zone Science* *Advancing Critical Zone*
871 *Science*. 2018.
- 872 Gleason, Sean M., Mark Westoby, Steven Jansen, Brendan Choat, Uwe G. Hacke, Robert B.

873 Pratt, Radika Bhaskar, Tim J. Brodribb, Sandra J. Bucci, Kun Fang Cao, Hervé Cochard,
874 Sylvain Delzon, Jean Christophe Domec, Ze Xin Fan, Taylor S. Feild, Anna L. Jacobsen,
875 Daniel M. Johnson, Frederic Lens, Hafiz Maherali, Jordi Martínez-Vilalta, Stefan Mayr,
876 Katherine A. McCulloh, Maurizio Mencuccini, Patrick J. Mitchell, Hugh Morris, Andrea
877 Nardini, Jarmila Pittermann, Lenka Plavcová, Stefan G. Schreiber, John S. Sperry, Ian J.
878 Wright, and Amy E. Zanne. “Weak Tradeoff between Xylem Safety and Xylem-Specific
879 Hydraulic Efficiency across the World’s Woody Plant Species.” *New Phytologist*
880 209(1):123–36. 2016.

881 Golaz, Jean-Christophe, Luke P. Van Roekel, Xue Zheng, Andrew F. Roberts, Jonathan D.
882 Wolfe, Wuyin Lin, Andrew M. Bradley et al. "The DOE E3SM Model Version 2: overview
883 of the physical model and initial model evaluation." *Journal of Advances in Modeling Earth*
884 *Systems* 14, no. 12 (2022).

885 Goulден, M L et al. “Evapotranspiration along an Elevation Gradient in California ’ s Sierra
886 Nevada.” *Journal of Geophysical Research* 117(1): 1–13. 2015.

887 Goulден, M L, and R C Bales. 2019. “California Forest Die-off Linked to Multi-Year Deep Soil
888 Drying in 2012–2015 Drought.” *Nature Geoscience* 12(August).
889 <http://dx.doi.org/10.1038/s41561-019-0388-5>.

890 Grime, J.P., Evidence for the existence of three primary strategies in plants and its relevance to
891 ecological and evolutionary theory. *The American Naturalist*, 111(982), pp.1169-1194.
892 1977.

893 Grime, J.P., Plant strategies and vegetation processes. *Plant strategies and vegetation processes*.
894 1979.

895 Hacke, Uwe G., Rachel Spicer, Stefan G. Schreiber, and Lenka Plavcová. “An Ecophysiological
896 and Developmental Perspective on Variation in Vessel Diameter.” *Plant Cell and*
897 *Environment* 40(6):831–45. 2017.

898 Hammond, W., K. Yu⁺, L. Wilson, R. Will, W.R.L. Anderegg, and H. Adams. 2019. “Dead or
899 dying? Quantifying the point of no return from hydraulic failure in drought-induced tree
900 mortality”. *New Phytologist*. doi: 10.1111/nph.15922. Published, 05/2019

901 Hartmann, Henrik, Waldemar Ziegler, Olaf Kolle, and Susan Trumbore. “Thirst Beats Hunger -
902 Declining Hydration during Drought Prevents Carbon Starvation in Norway Spruce
903 Saplings.” *New Phytologist* 200(2):340–49. 2013.

904 Hartung, Wolfram, Angela Sauter, and Eleonore Hose. “Abscisic Acid in the Xylem : Where
905 Does It Come from , Where Does It Go To ?” 53(366): 27–32. 2002.

906 Hetherington, Alistair M, and F Ian Woodward. “The Role of Stomata in Sensing and Driving
907 Environmental Change.” *Nature* 424(August): 901–8. 2003.

908 Huang, J., Kautz, M., Trowbridge, A. M., Hammerbacher, A., Raffa, K. F., Adams, H. D., ... &
909 Gershenson, J. Tree defence and bark beetles in a drying world: carbon partitioning,
910 functioning and modelling. *New Phytologist*, 225(1), 26-36. (2020).

911 Inouea, Shin-ichiro, and Toshinori Kinoshitaa. 2017. “Blue Light Regulation of Stomatal
912 Opening and the Plasma Membrane H⁺-ATPase 2.” *Plant Physiology* (166): 17.

- 913 Ivanov, Valeriy Y., Lucy R. Hutyrá, Steven C. Wofsy, J. William Munger, Scott R. Saleska,
914 Raimundo C. De Oliveira, and Plínio B. De Camargo. “Root Niche Separation Can Explain
915 Avoidance of Seasonal Drought Stress and Vulnerability of Overstory Trees to Extended
916 Drought in a Mature Amazonian Forest.” *Water Resources Research* 48(12):1–21. 2012.
- 917 Jackson, R.B., Canadell, J., Ehleringer, J.R., Mooney, H.A., Sala, O.E. and Schulze, E.D., A
918 global analysis of root distributions for terrestrial biomes. *Oecologia*, 108(3), pp.389-411.
919 1996.
- 920 Johnson, D. M., Domec, J. C., Carter Berry, Z., Schwantes, A. M., McCulloh, K. A., Woodruff,
921 D. R., ... & McDowell, N. G. Co-occurring woody species have diverse hydraulic strategies
922 and mortality rates during an extreme drought. *Plant, Cell & Environment*, 41(3), 576-588.
923 2018.
- 924 Kattge, J., Bönišch, G., Díaz, S., Lavorel, S., Prentice, I. C., Leadley, P., Tautenhahn, S., Werner,
925 G., et al. “TRY Plant Trait Database - Enhanced Coverage and Open Access.” *Global
926 Change Biology* 26(1):119–88. 2020.
- 927 Kelly, Anne E, and Michael L Goulden. “A Montane Mediterranean Climate Supports Year-
928 Round Photosynthesis and High Forest Biomass.” : 459–68. 2016.
- 929 Khasanova, Albina, John T. Lovell, Jason Bonnette, Xiaoyu Weng, Jerry Jenkins, Yuko
930 Yoshinaga, Jeremy Schmutz, and Thomas E. Juenger. “The Genetic Architecture of Shoot
931 and Root Trait Divergence between Mesic and Xeric Ecotypes of a Perennial Grass.”
932 *Frontiers in Plant Science* 10(April):1–10. 2019.
- 933 Kilgore, J.S., Jacobsen, A.L. and Telewski, F.W., Hydraulics of Pinus (subsection Ponderosae)
934 populations across an elevation gradient in the Santa Catalina Mountains of southern
935 Arizona. *Madroño*, 67(4), pp.218-226. 2021.
- 936 Klos, P Zion et al. “Subsurface Plant-Accessible Water in Mountain Ecosystems with a
937 Mediterranean Climate.” *Wiley Interdisciplinary Reviews: Water* (May 2017): 1–14. 2017.
- 938 Koch, G.W. and Fredeen, A.L., Transport challenges in tall trees. In *Vascular transport in
939 plants* (pp. 437-456). Academic Press. 2005.
- 940 Koven, C.D., Knox, R.G., Fisher, R.A., Chambers, J.Q., Christoffersen, B.O., Davies, S.J.,
941 Detto, M., Dietze, M.C., Faybishenko, B., Holm, J. and Huang, M., Benchmarking and
942 parameter sensitivity of physiological and vegetation dynamics using the Functionally
943 Assembled Terrestrial Ecosystem Simulator (FATES) at Barro Colorado Island,
944 Panama. *Biogeosciences*, 17(11), pp.3017-3044. 2020.
- 945 Kulmatiski, Andrew and Karen H. Beard. “Root Niche Partitioning among Grasses, Saplings,
946 and Trees Measured Using a Tracer Technique.” *Oecologia* 171(1):25–37. 2013.
- 947 Lawrence, D.M., Fisher, R.A., Koven, C.D., Oleson, K.W., Swenson, S.C., Bonan, G., Collier,
948 N., Ghimire, B., van Kampenhout, L., Kennedy, D. and Kluzek, E., The Community Land
949 Model version 5: Description of new features, benchmarking, and impact of forcing
950 uncertainty. *Journal of Advances in Modeling Earth Systems*, 11(12), pp.4245-4287.
- 951 Li, S., Lens, F., Espino, S., Karimi, Z., Klepsch, M., Schenk, H.J., Schmitt, M., Schuldt, B. and

- 952 Jansen, S., 2016. Intervessel pit membrane thickness as a key determinant of embolism
953 resistance in angiosperm xylem. *Iawa Journal*, 37(2), pp.152-171. 2019.
- 954 Lu, Yaojie et al. 2019. “Optimal Stomatal Drought Response Shaped by Competition for Water
955 and Hydraulic Risk Can Explain Plant Trait Covariation.” (1977).
- 956 Mackay, D. S., Savoy, P. R., Grossiord, C., Tai, X., Pleban, J. R., Wang, D. R., ... & Sperry, J. S.
957 Conifers depend on established roots during drought: results from a coupled model of
958 carbon allocation and hydraulics. *New Phytologist*, 225(2), 679-692. 2020.
- 959 Martínez-Vilalta, Jordi, Anna Sala, and Josep Piñol. *The Hydraulic Architecture of Pinaceae-a*
960 *Review*. Vol. 171. 2004.
- 961 Matheny, Ashley M, Golnazalsadat Mirfenderesgi, and Gil Bohrer. “Trait-Based Representation
962 of Hydrological Functional Properties of Plants in Weather and Ecosystem Models.” *Plant*
963 *Diversity* 39(1): 1–12. <http://dx.doi.org/10.1016/j.pld.2016.10.001>. 2017.
- 964 Matheny, A.M., Fiorella, R.P., Bohrer, G., Poulsen, C.J., Morin, T.H., Wunderlich, A., Vogel,
965 C.S. and Curtis, P.S., Contrasting strategies of hydraulic control in two codominant
966 temperate tree species. *Ecology*, 10(3), p.e1815. 2017.
- 967 McDowell, Nate, Nate McDowell, William T. Pockman, Craig D. Allen, D. David, Neil Cobb,
968 Thomas Kolb, Jennifer Plaut, John Sperry, Adam West, David G. Williams, and Enrico A.
969 Yezzer. “Mechanisms of Plant Survival and Mortality during Drought : Why Do Some
970 Plants Survive While Others Succumb To.” 2008.
- 971 McDowell, Nate G. et al. “Evaluating Theories of Drought-Induced Vegetation Mortality Using
972 a Multimodel – Experiment Framework.” : 304–21. 2013.
- 973 Mooney, Harold and Erika Zavaleta. *Ecosystems of California*. Vol. 3. edited by H. Mooney and
974 E. Zavaleta. Oakland, California, USA: Univ of California Press. 2003.
- 975 Mursinna, A. Rio, Erica McCormick, Kati Van Horn, Lisa Sartin, and Ashley M. Matheny.
976 “Plant Hydraulic Trait Covariation: A Global Meta-Analysis to Reduce Degrees of Freedom
977 in Trait-Based Hydrologic Models.” *Forests* 9(8). 2018.
- 978 Oleson, Keith W et al. “Technical Description of Version 4.5 of the Community Land Model
979 (CLM) Coordinating.” In *Natl. Cent. Atmos. Res. Tech. Note*, Natl. Cent. for Atmos. Res.,
980 Boulder, Colo. 2013.
- 981 Pittermann, Jarmila, John S. Sperry, Uwe G. Hacke, James K. Wheeler, and Elzard H. Sikkema.
982 “Inter-Tracheid Pitting and the Hydraulic Efficiency of Conifer Wood: The Role of
983 Tracheid Allometry and Cavitation Protection.” *American Journal of Botany* 93(9):1265–
984 73. 2006.
- 985 Pittermann, Jarmila, John S. Sperry, James K. Wheeler, Uwe G. Hacke, and Elzard H. Sikkema.
986 “Mechanical Reinforcement of Tracheids Compromises the Hydraulic Efficiency of Conifer
987 Xylem.” *Plant, Cell and Environment* 29(8):1618–28. 2006.
- 988 Pockman, W.T. and Sperry, J.S., Vulnerability to xylem cavitation and the distribution of
989 Sonoran desert vegetation. *American journal of botany*, 87(9), pp.1287-1299. 2000.

- 990 Powell, Thomas L., James K. Wheeler, Alex A. R. de Oliveira, Antonio Carlos Lola da Costa,
991 Scott R. Saleska, Patrick Meir, and Paul R. Moorcroft. "Differences in Xylem and Leaf
992 Hydraulic Traits Explain Differences in Drought Tolerance among Mature Amazon
993 Rainforest Trees." *Global Change Biology* 23(10):4280–93. 2017.
- 994 Pratt, R.B. and Jacobsen, A.L., Conflicting demands on angiosperm xylem: tradeoffs among
995 storage, transport and biomechanics. *Plant, Cell & Environment*, 40(6), pp.897-913. 2017.
- 996 Reich, Peter B., Ian J. Wright, Jeannine Cavender-Bares, J. M. Craine, Jacek Oleksyn, M.
997 Westoby, and M. B. Walters. "The evolution of plant functional variation: traits, spectra,
998 and strategies." *International Journal of Plant Sciences* 164, no. S3: S143-S164. (2003).
- 999 Reichstein, M., Bahn, M., Mahecha, M.D., Kattge, J. and Baldocchi, D.D., Linking plant and
1000 ecosystem functional biogeography. *Proceedings of the National Academy of
1001 Sciences*, 111(38), pp.13697-13702. 2014.
- 1002 Rodriguez-Dominguez, C.M., Buckley, T.N., Egea, G., de Cires, A., Hernandez-Santana, V.,
1003 Martorell, S. and Diaz-Espejo, A., Most stomatal closure in woody species under moderate
1004 drought can be explained by stomatal responses to leaf turgor. *Plant, Cell &
1005 Environment*, 39(9), pp.2014-2026. 2016.
- 1006 Rowland, L., A. C. L. Da Costa, D. R. Galbraith, R. S. Oliveira, O. J. Binks, A. A. R. Oliveira,
1007 A. M. Pullen, C. E. Doughty, D. B. Metcalfe, S. S. Vasconcelos, L. V. Ferreira, Y. Malhi, J.
1008 Grace, M. Mencuccini, and P. Meir. "Death from Drought in Tropical Forests Is Triggered
1009 by Hydraulics Not Carbon Starvation." *Nature* 528(7580):119–22. 2015.
- 1010 Salmon, Yann, José M. Torres-Ruiz, Rafael Poyatos, Jordi Martinez-Vilalta, Patrick Meir, Hervé
1011 Cochard, and Maurizio Mencuccini. "Balancing the Risks of Hydraulic Failure and Carbon
1012 Starvation: A Twig Scale Analysis in Declining Scots Pine." *Plant Cell and Environment*
1013 38(12):2575–88. 2015.
- 1014 Sauter, Angela, W J Davies, Wolfram Hartung, and Lehrstuhl Botanik I. "The Long-Distance
1015 Abscisic Acid Signal in the Droughted Plant : The Fate of the Hormone on Its Way from
1016 Root to Shoot." 52(363): 1991–97. 2001.
- 1017 Skelton, R. P., West, A. G., & Dawson, T. E. "Predicting plant vulnerability to drought in
1018 biodiverse regions using functional traits." *Proceedings of the National Academy of
1019 Sciences*, 112(18), 5744-5749. 2015.
- 1020 Sevanto, Sanna, Nate G. McDowell, L. Turin Dickman, Robert Pangle, and William T. Pockman.
1021 "How Do Trees Die? A Test of the Hydraulic Failure and Carbon Starvation Hypotheses."
1022 *Plant, Cell and Environment* 37(1):153–61. 2014.
- 1023 Sperry, John S. "Evolution of Water Transport and Xylem Structure." *International Journal of
1024 Plant Sciences* 164. 2003.
- 1025 Teuling, Adriaan J, Remko Uijlenhoet, and Peter A Troch. "Impact of Plant Water Uptake
1026 Strategy on Soil Moisture and Evapotranspiration Dynamics during Drydown." 33: 3–7.
1027 2006.
- 1028 Vesala, T., Sevanto, S., Grönholm, T., Salmon, Y., Nikinmaa, E., Hari, P. and Hölttä, T., Effect

- 1029 of leaf water potential on internal humidity and CO₂ dissolution: reverse transpiration and
1030 improved water use efficiency under negative pressure. *Frontiers in plant science*, 8, p.54.
1031 2017.
- 1032 Westoby, M., Falster, D.S., Moles, A.T., Vesk, P.A. and Wright, I.J., Plant ecological strategies:
1033 some leading dimensions of variation between species. *Annual review of ecology and*
1034 *systematics*, 33(1), pp.125-159. 2002.
- 1035 Wilkinson, S, and W J Davies. “ABA-Based Chemical Signalling : The Co-Ordination Of.” :
1036 195–210. 2002.
- 1037 Wullschleger, Stan D. et al. “Plant Functional Types in Earth System Models : Past Experiences
1038 and Future Directions for Application of Dynamic Vegetation Models in High-Latitude
1039 Ecosystems.” *Annals of botany* (114): 1–16. 2014.
- 1040 Yu, Gui-rui, Jie Zhuang, and Keiichi Nakayamma. “Root Water Uptake and Profile Soil Water
1041 as Affected by Vertical Root Distribution.” *Plant Ecol*: 15–30. 2007.
- 1042 Zeng, Xubin. “Global Vegetation Root Distribution for Land Modeling.” *Journal of*
1043 *Hydrometeorology* 2(5): 525–30. 2001.
- 1044
- 1045

1046 **Tables**

1047 **Table 1 Parameters used in FATES-Hydro sensitivity analysis**

1048

Parameters	Biological meaning	Values	Units
r_a, r_b	Root distribution: shallow roots vs. deep roots	(0.1, 0.1) – (2 5)	unitless
$P50_{gs}$	Leaf xylem water potential at half stomatal closure stomatal control on safety vs. efficiency	$P50_x - P20_x$	Mpa
$P50_x$	Xylem water potential when xylem loss half of the conductance	-3.0 ^a , -4.8 ^b	Mpa
K_{max}	Maximum xylem conductivity per unit sap area	0.88 ^a , 0.64 ^b	kg/MPa/m/s
A	Shape parameter of van Genuchten hydrologic function	0.11855 ^a , 0.088026 ^b	Mpa ⁻¹
m, n	Shape parameters of van Genuchten hydrologic function	(0.8, 1.25) ^a , (0.8, 1.5) ^b	unitless

1049 a: values for efficient/unsafe xylem

1050 b: values for inefficient/safe xylem

1051

Table 2. List of major parameters

Symbol	Source code name	Value	Units	Description	Source
a_{gs}	fates_hydr_avuln_gs	2.5	unitless	shape parameter for stomatal control of water vapor (slope) exiting leaf	Christoffersen et al., 2016
χ	fates_hydr_p_taper	0.333	unitless	xylem taper exponent	Christoffersen et al., 2016
$\pi_{o,l}, \pi_{o,s}, \pi_{o,r}$	fates_hydr_pinot_node	-1.47, -1.23, -1.04	MPa	osmotic potential at full turgor of leaf, stem, root	Christoffersen et al., 2016
$RWC_{res,l}, RWC_{res,s}, RWC_{res,r}$	fates_hydr_resid_node	0.25, 0.325, 0.15	proportion	residual fraction of leaf, stem, root	Christoffersen et al., 2016
$\Theta_{sat,x}$	fates_hydr_thetas_node	0.65	cm ³ /cm ³	saturated water content of xylem	Christoffersen et al., 2016
SLA_{max}	fates_leaf_slamax	0.01	m ² /gC	Maximum Specific Leaf Area (SLA)	TRY
SLA_{top}	fates_leaf_slatop	0.01	m ² /gC	Specific Leaf Area (SLA) at top of canopy, projected area basis	TRY
$V_{cmax,25, top}$	fates_leaf_vcmax25top	55	umol CO ₂ /m ² /s	maximum carboxylation rate of Rub. at 25C, canopy top	TRY
b_{opt}	fates_bbopt_c3	10000	umol H ₂ O/m ² /s	Ball-Berry minimum leaf stomatal conductance for C3 plants	Calibrated

Figures

Figure 1

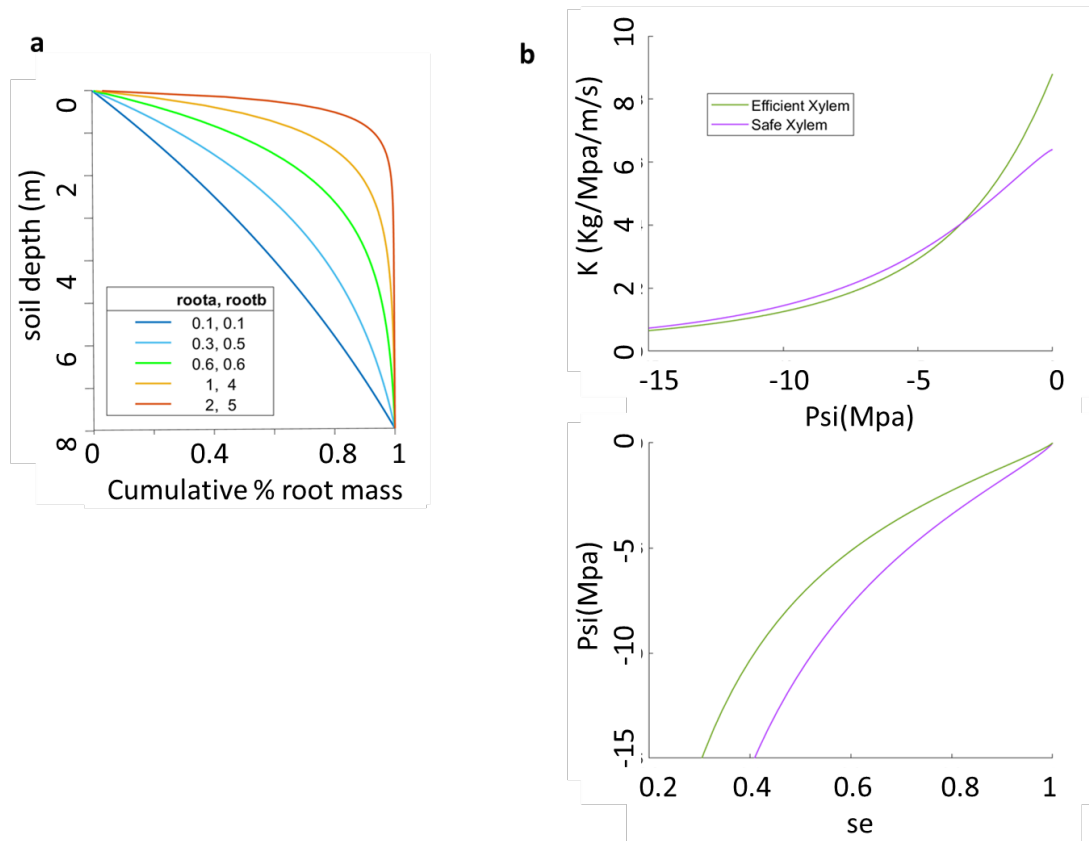


Figure 1. Sensitivity analysis set up for: a) root parameters that give five root distribution scenarios with effective rooting depths of 1m, 3m, 5m, 6.5m, and 8m , and b) two xylem scenarios for safe xylem ($P50x=-4.8$, $K_{max}=0.64$), and efficient xylem ($P50x=-2.5$, $K_{max}=0.88$).

Figure 2

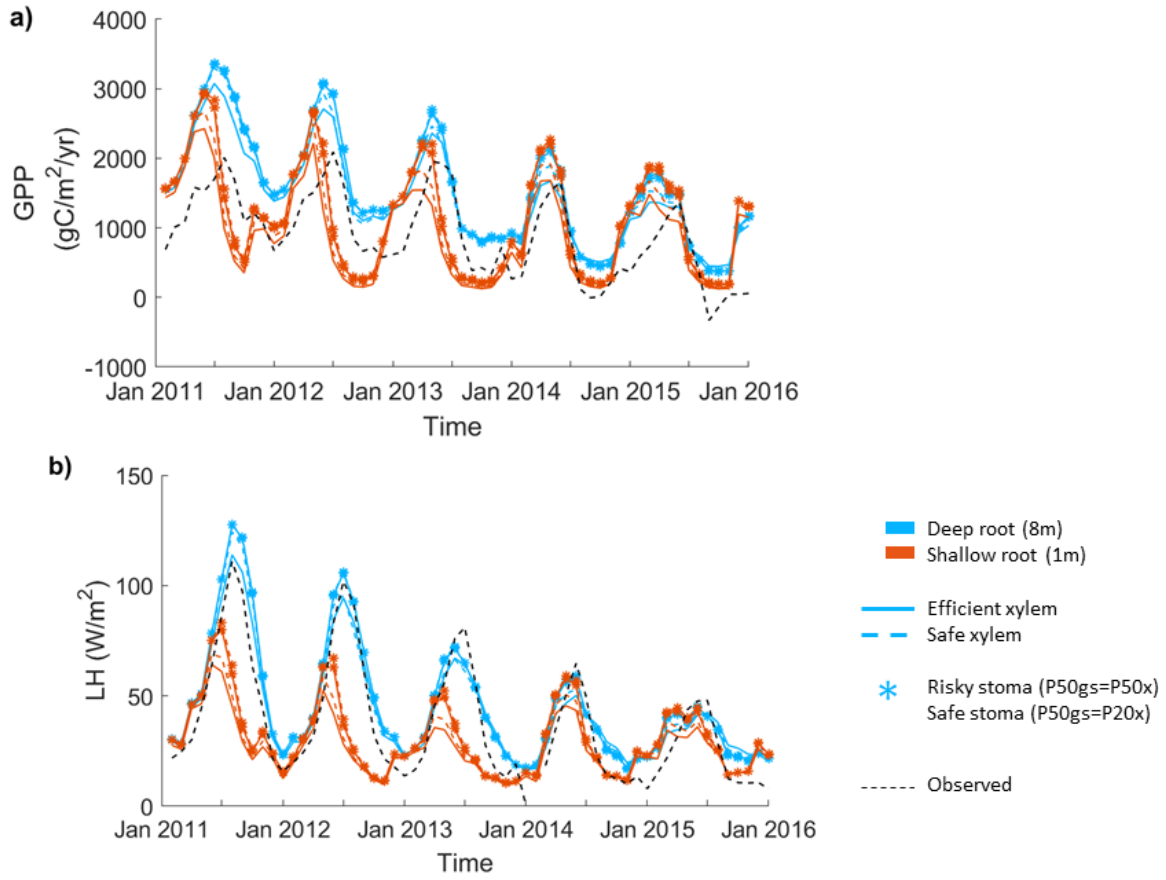


Figure 2. Impact of hydraulic strategies on ecosystem water and energy fluxes: a) monthly mean gross primary productivity, and B) monthly mean latent heat flux, of the end member cases.

Figure 3

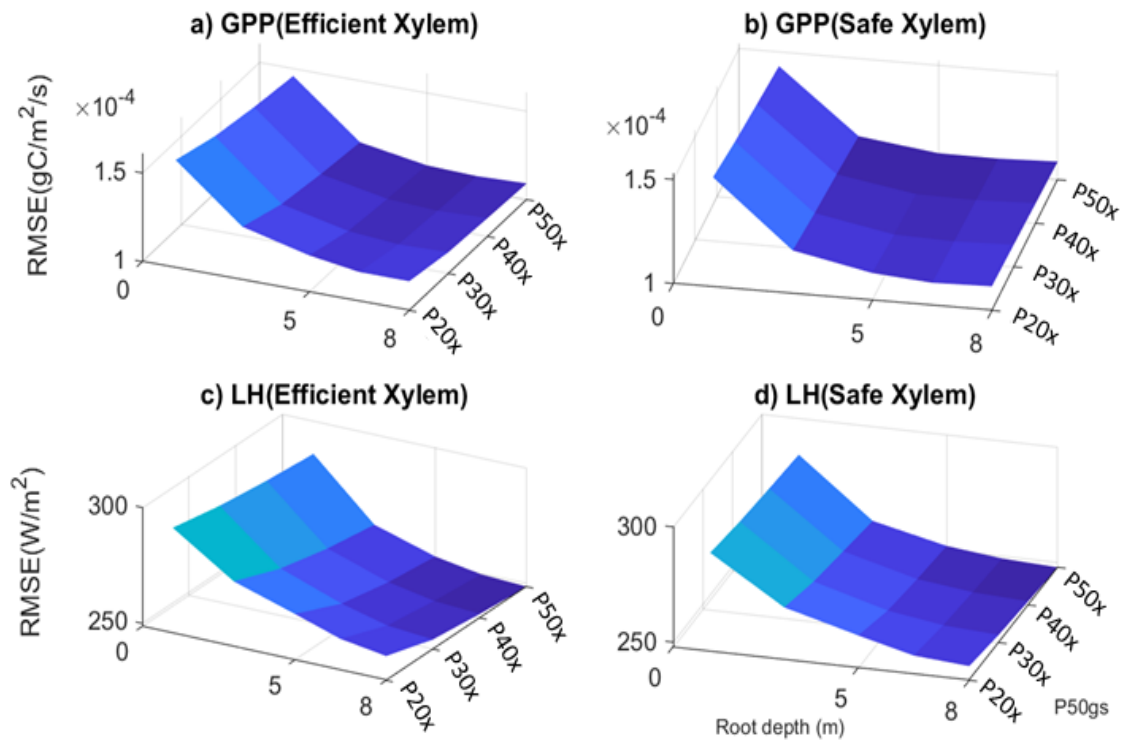


Figure 3. Root mean square error of GPP (a-b), and latent heat flux (c-d) with respect to variation in input parameters.

Figure 4

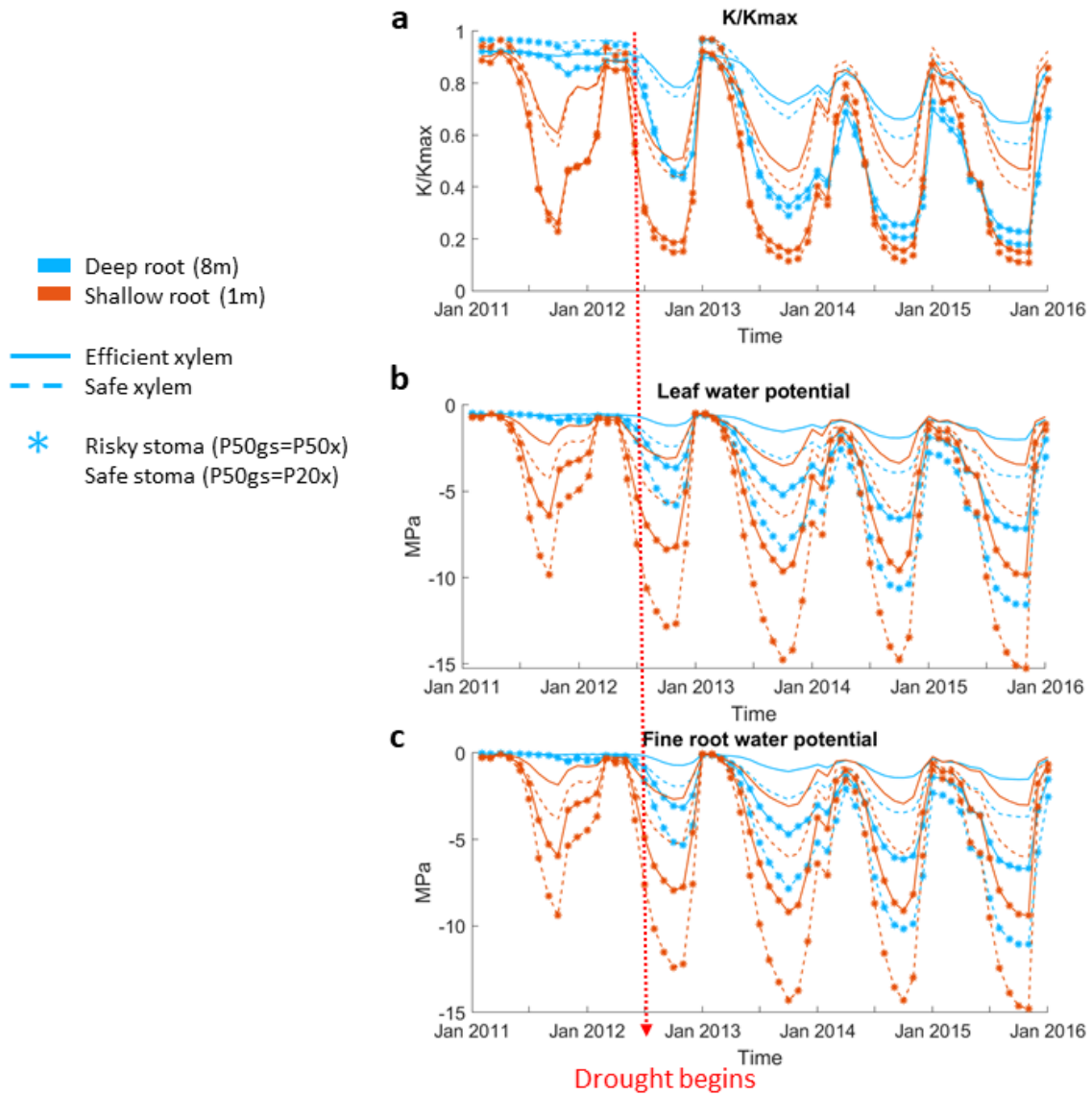


Figure 4. Seasonal and inter-annual variation of plant physiologic characteristics: a) monthly mean stem fraction of conductance K/K_{max} (a), monthly mean leaf water potential, and c) monthly mean overall absorbing roots water potential, of the 55cm DBH cohort throughout the 2011-2015 period.

Figure 5

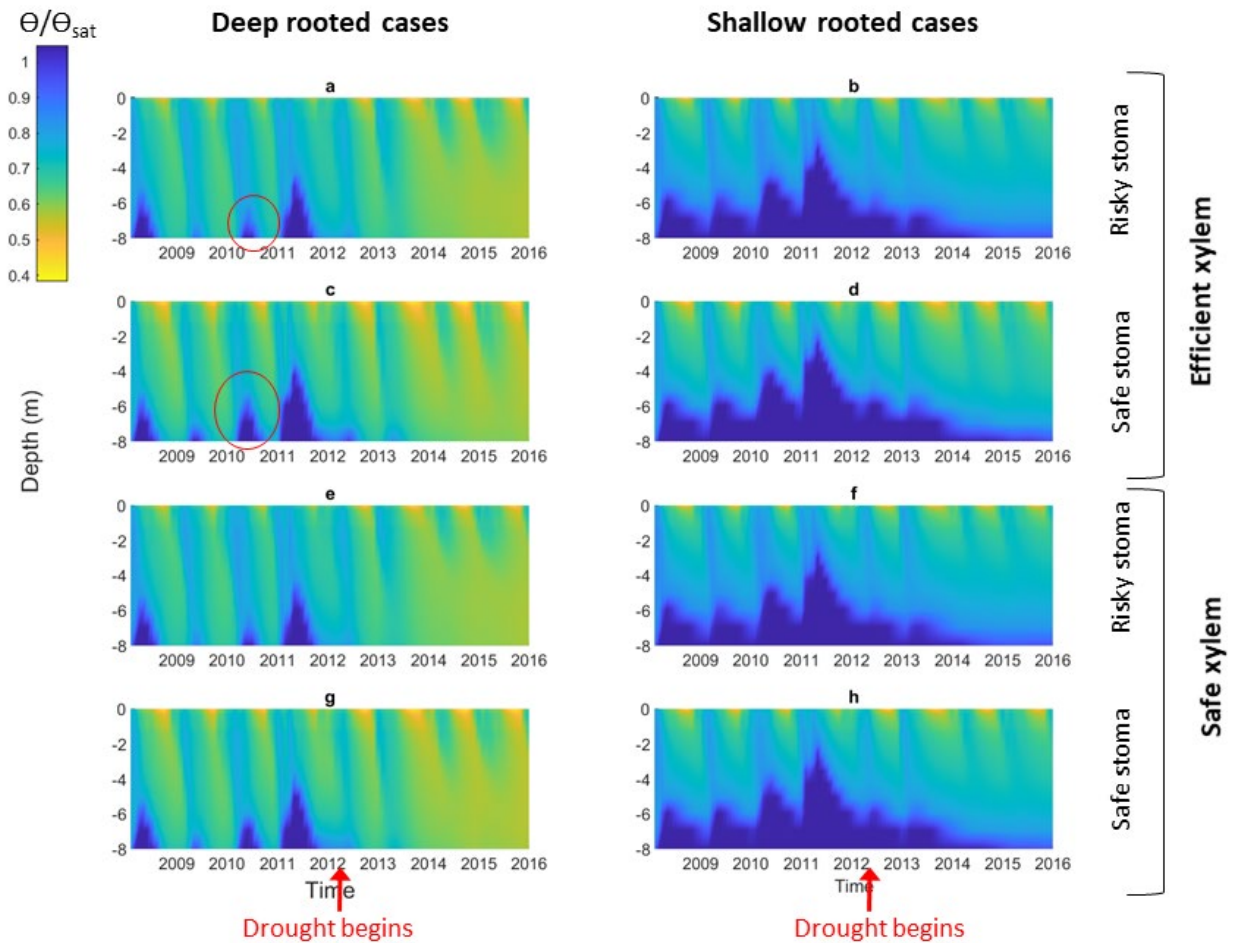


Figure 5. Impact of different combination of rooting depth, xylem and stomatal traits on soil moisture; left column shows deep rooted cases with a) efficient xylem and risky stoma, c) efficient xylem and safe stoma, e) safe xylem and risky stoma, g) safe xylem and safe stoma. Right column shows shallow rooted cases with b) efficient xylem and risky stoma, d) efficient xylem and safe stoma, f) safe xylem and risky stoma, h) safe xylem and safe stoma; red cycle highlights the effect of stomatal traits on deep water storage during the wet season of the pre-drought period

Figure 6

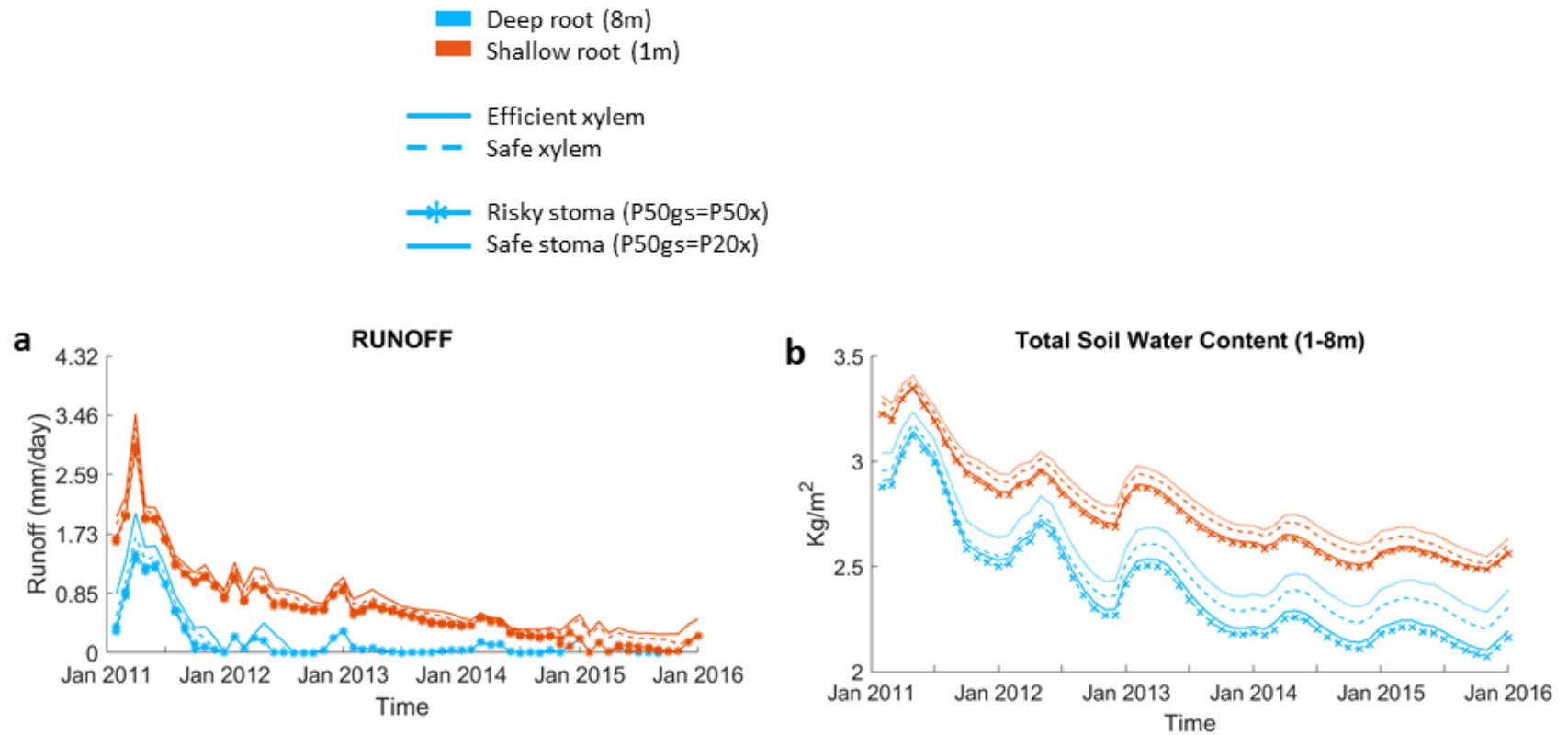


Figure 6. Impact on hydrologic processes: a) mean monthly total runoff, and b) monthly mean total soil water content of the entire soil column.

Figure 7

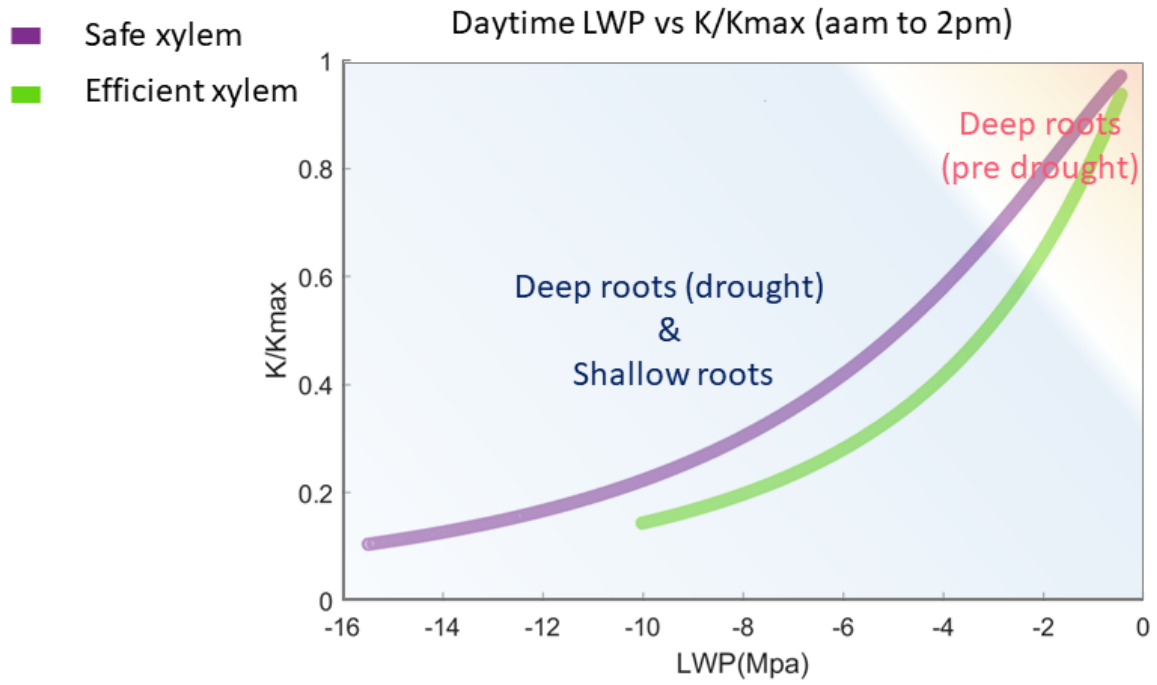


Figure 7. Simulated leaf water potential and fraction loss of conductivity (K/K_{max}) of all the cases, which follow the two vulnerability curves.

Figure 8

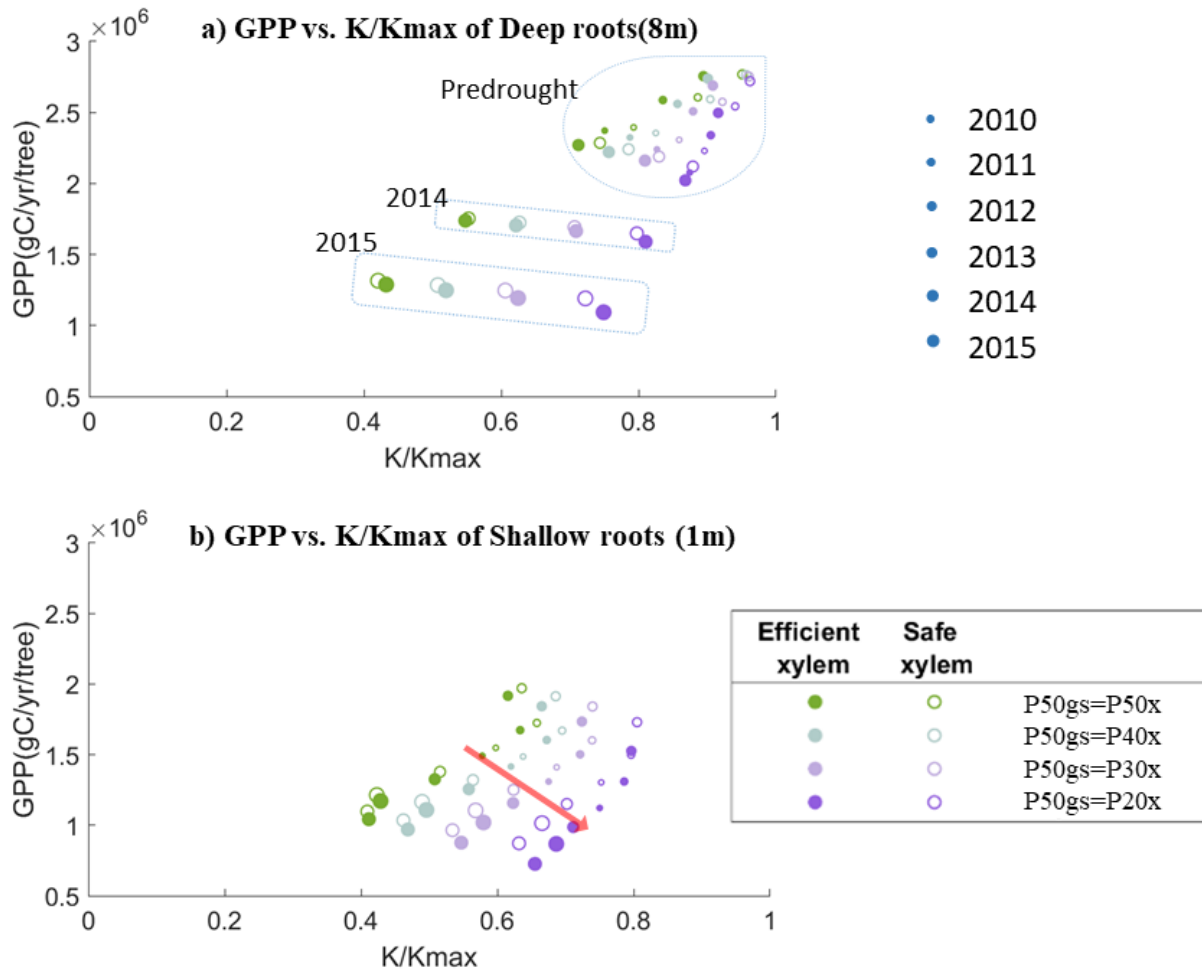


Figure 8. Simulated average annual GPP and fraction of conductance of a 55cm DBH cohort with a) deep roots (effective rooting depth= 8m) and b) shallow roots (effective rooting depth= 1m).